AD-A035 594 ARMY ELECTRONICS COMMAND FORT MONMOUTH N J F/G 20/5
DEVELOPMENT OF SPECTROPHONES FOR CW AND PULSED RADIATION SOURCE--ETC(U)
AUG 76 C BRUCE

UNCLASSIFIED ECOM-5802 NL

1 OF 1
ADA035594

END

DATE
FILMED
3-77

RESEARCH AND DEVELOPMENT TECHNICAL REPORT
ECOM-5802

DEVELOPMENT OF SPECTROPHONES FOR CW AND PULSED RADIATION SOURCES

By

Charles Bruce

Atmospheric Sciences Laboratory
US Army Electronics Command
White Sands Missile Range, New Mexico 88002

August 1976

ECOM
UNITED STATES ARMY ELECTRONICS COMMAND - FORT MONMOUTH, NEW JERSEY 07703

NOTICES

Disclaimers

The findings in this report are not to be construed as an official Department of the Army position, unless so designated by other authorized documents.

The citation of trade names and names of manufacturers in this report is not to be construed as official Government indorsement or approval of commercial products or services referenced herein.

Disposition

Destory this report when it is no longer needed. Do not return it to the originator.

SECURITY CLASSIFICATION OF THIS PAGE (When Data Entered)

(14)

REPORT DOCUMENTATION PAGE

READ INSTRUCTIONS BEFORE COMPLETING FORM

1. REPORT NUMBER: ECOM-5802 (9) Research and development technical rept.)	2. GOVT ACCESSION NO. / 3. RECIPIENT'S CATALOG NUMBER
(6) 4. TITLE (and Subtitle): DEVELOPMENT OF SPECTROPHONES FOR CW AND PULSED RADIATION SOURCES.	5. TYPE OF REPORT & PERIOD COVERED
	6. PERFORMING ORG. REPORT NUMBER
(10) 7. AUTHOR(s): Charles Bruce	8. CONTRACT OR GRANT NUMBER(s)
9. PERFORMING ORGANIZATION NAME AND ADDRESS: Atmospheric Sciences Laboratory, White Sands Missile Range, New Mexico 88002	10. PROGRAM ELEMENT, PROJECT, TASK AREA & WORK UNIT NUMBERS: DA Task No. 822000.8T52943
11. CONTROLLING OFFICE NAME AND ADDRESS: US Army Electronics Command, Fort Monmouth, New Jersey 07703 (11)	12. REPORT DATE: August 1976 (12) 63p.
	13. NUMBER OF PAGES: 68
14. MONITORING AGENCY NAME & ADDRESS (if different from Controlling Office)	15. SECURITY CLASS. (of this report): UNCLASSIFIED
	15a. DECLASSIFICATION/DOWNGRADING SCHEDULE

16. DISTRIBUTION STATEMENT (of this Report)

Approved for public release; distribution unlimited.

17. DISTRIBUTION STATEMENT (of the abstract entered in Block 20, if different from Report)

18. SUPPLEMENTARY NOTES

19. KEY WORDS (Continue on reverse side if necessary and identify by block number)

Opto-acoustical sensors	Lasers
Spectrophones	Pulsed lasers
Atmospheric absorption	CW lasers
IR transmission	

20. ABSTRACT (Continue on reverse side if necessary and identify by block number)

This technical report describes the construction of high sensitivity absorption measurement systems based on spectrophones (opto-acoustical cells) which have been developed for both CW and pulsed laser sources. These systems have been applied to measurements of absorption by atmospheric gases and particulates at IR laser frequencies. Construction, calibration, and linearity are discussed for a number of specific systems.

Accurate measurements of absorption by atmospheric constituents in the so-called

over

DD FORM 1 JAN 73 1473 EDITION OF 1 NOV 65 IS OBSOLETE

037620

SECURITY CLASSIFICATION OF THIS PAGE (When Data Entered)

20. ABSTRACT (cont)

transmission "window" frequency bands are required by both the DoD high-energy laser (HEL) and electro-optical sensor programs. Statistical predictions for system design and the development of real-time field measurement systems are both important possible applications of spectrophones of the type discussed in this report. High sensitivity is generally a requirement as a result of the relatively low absorption in the "windows."

CONTENTS

INTRODUCTION

Interest in the high resolution spectroscopy of molecules appearing in the atmosphere has recently been spurred by proposed long path transmission applications of IR lasers. The development of a veritable catalogue of IR lasers allows selection within transmission "windows," but because of the anticipated long paths, predictions require high accuracy for relatively small absorption coefficients.

Due to complex dependence of the spectra on thermodynamic variables, the variability of the constituent proportions, and unidentified losses due to particulates, measurements must be performed in a controlled environment. In other words, laboratory systems of high purity must be used to identify the absorption coefficients individually as broadened by the major atmospheric constituents. This method provides information for molecular models as well as transmission predictions.

High resolution systems capable of measuring absorption coefficients as low as 0.1 km^{-1} with sufficient accuracy have, until this decade, been limited primarily to long path transmission cells. Generally, these use beam folding optics to multiply optical path length by as much as two orders of magnitude. Such "White" cell systems must have high vacuum integrity, be bakeable, temperature controlled, and have high quality (and large) optics. Inevitably, long path transmission cells are ponderous, complex, and expensive. Furthermore, absorption coefficients for transmission favored "windows" are frequently considerably less than 0.1 km^{-1}, stressing White cell accuracy beyond acceptable limits. Here the subtraction (of transmittance) from unity required to obtain the absorbance results in a much higher percentage error for the latter quantity than for the measured transmittance. Some simpler measurement of a quantity directly proportional to the absorbance or absorption coefficient itself would be desirable.

A direct and convenient mechanism resulting from IR photon absorption is that increased energy in the molecular rotation/vibration structure generally appears in translational (kinetic) form in the equilibration process. Thus measurement of thermodynamic properties of the gas might be expected to provide a proportional measure of the absorbed energy. Although there are exceptions (involving, e.g., energy trapped in metastable states or reradiation), they are expected to be infrequent in these applications. Actually this measurement concept was stated nearly a century ago [1,2] and the measurement device appropriately named "spectrophone" as suggested by Alexander Graham Bell [1].

Applications using laser sources first appeared in 1968 [3], but these were clearly exploratory and did not represent measurements of precision.

Two major categories of such devices appeared in the literature in the early 1970's, both using CW lasers and beam "chopping" devices (time gating). One category involves the use of pressure sensors, such as capacitance manometers and very slow chopping rates (usually less than 1 Hz) to obtain an equilibrium [4]. A second category involves use of microphone sensors and considerably higher chopping rates which excite acoustic waves emanating from the absorbing region [5]. In the second category, a resonant cavity may or may not be employed [6].

Though a number of publications have appeared regarding spectrophone use [7-9], development of these devices is still at an early stage. For example, the particular spectrophone design and technique does not always appear to suit the application. In other instances a limitation of the measurement will have been incorrectly considered inherent to the technique. These points will be discussed in this report.

The spectrophone developments reported here represent applications of spectrophones in several areas and incorporation of new ideas in some cases and new applications for measurement quality devices in others.

CW SOURCE SPECTROPHONE DESIGN CONSIDERATIONS

Required Qualities

At the start of this work in mid-1974, it was clear that the ideal system would be required to have the following properties:

1. Sensitivity: absorption coefficients smaller than 10^{-3} km^{-1} measurable

2. Power linearity of absorption signal

3. Single measurement precision: within 10% of mean at 10^{-3} km^{-1}

4. Stability: negligible drift or jitter for duration of complete series of measurements (determined from multimeasurement average)

Sensitivity for spectrophones is limited by noise and signal components not directly associated with the gaseous absorption. This sensitivity is very much dependent on physical design, sensor type and, most important, signal processing. Since the directness of the approach and earlier work have made clear the generally high level of sensitivity [5,6,10,11], this issue will not be discussed extensively here.

The question of signal linearity with power is important and somewhat involved. For the IR absorption processes of interest, transitions occur between particular rotational levels of two vibrational levels. The

lower vibrational level is generally, but not necessarily, the ground state. It should also be noted that for molecular absorbers whose energy levels are broadened as in the lower atmosphere, a great deal of "overlap" between lines occurs. For a single absorber, line separation varies from less than 1 cm^{-1} to just over 10 cm^{-1} with most atmospheric absorbers tending to the small values. Atmospheric line widths (STP, FWHM) are of the order of 10^{-1} cm^{-1}. Still, even for a single absorber, total overlap or probabilistic coincidence can be significant, particularly when adjacent line strengths are relatively high.

Although exceptions have been reported [12,13], for the following discussion it will be assumed that the individual lines contribute to the absorption coefficient additively.

The change in thermodynamic parameters due to molecular absorption of a continued photon flux can be approached through the application of the rate equation for the change in the upper state density with time. This equation is composed of excitation terms for transition rates to the upper state as induced by collisions in the gas and photon flux and de-excitation terms for both of these and another for spontaneous decay.

With terms in the same order and with the appropriate coefficients or induced and spontaneous transitions included, the equation reads

$$\dot{\rho}_2 = I\rho_1 k + f_{12}\rho_1 - (I\rho_2 k + f_{21}\rho_2 + f_2\rho_2). \qquad (1)$$

Here I represents the photon flux density and the subscripts 2 and 1 refer to the upper and lower states, respectively. Since the collisional energy for the conditions of interest is much less in the mean than that of the separation of vibrational states, photon excitation predominates.

Using the total density, $\rho = \rho_1 + \rho_2$, Eq. (1) becomes

$$\dot{\rho}_2 \cong I\rho k - \rho_2(f_{21} + f_2 + 2Ik)$$

$$= I\rho k - \rho_2(f). \qquad (2)$$

The spontaneous relaxation rate is several orders of magnitude smaller than the collision de-excitation rate for all known cases of interest. The solution (particular plus general) is

$$\rho_2 = I\rho kf + ce^{-\rho_2 f} \qquad (3)$$

and the long-term solution is then

$$\rho_2 \cong I\rho k/f = \frac{I\rho k}{f_{21} + 2Ik} . \qquad (4)$$

The equation shows that the upper state population will be directly related to the intensity of the illuminating beam if $f_{21} >> 2Ik$. In practice, the collision frequency is sufficiently high and the induced de-excitation rates small enough that this linearity may easily be maintained. If the molecular system is saturated however, i.e., if the frequency of induced transitions is much larger than the collision frequency, the upper state population becomes independent of the intensity (at the level $\rho/2$).

If the intensity is modulated, linearity of the upper state population with respect to intensity may still be maintained. The conditions are: (a) the previously mentioned dc condition and (b) the system response requirement that the frequency represented by the quantity f is much greater than the driving frequency.

The increase in translational energy and thus the pressure is then proportional to the increased population density of the upper state. Thermodynamic equilibrium is established through the loss to the container walls. Since the effective relaxation time constant for the latter process is relatively long, the loss rate is relatively low.

The properties of precision and stability are included for completeness but do not require further explanation here. These concerns are implicit in the discussions to follow on specific designs.

Whatever design prospects were indicated by the requirements, the most decisive factors lay in the desirable facets for high sensitivity measurement systems.

Desired Qualities

1. Signal to noise (S/N): Choice of passband center frequency remains an option, while passband width should be approximately zero.

a. Option 1. Passband at $f \cong 0$ allows use of dc pressure sensors but also permits drift due to thermal fluctuations in the cell walls or appendages and pressure sensor, window heating, and electrical system drift all to contribute to the noise. Averaging over many "cycles" of a chopped CW beam may be performed.

b. Option 2. Passband in the acoustical sensor range eliminates drift due to both thermal and electrical sources (using ac techniques). Line and high frequency electrical noise must be avoided and photon absorption to translational relaxation rate should significantly exceed the operating frequency.

2. Incorporation of acoustic gain if possible. Use of "Q" is roughly equivalent to a very selective preamplifier, i.e., gain (but not constant) over a limited bandwidth.

3. Removal of window source signal without sensitive balance procedures (including contributions of particles and imperfections in or on windows).

4. Operational simplicity without sacrifice of essential qualities.

5. Capability of operation in a flow-through mode (absorption measurements of continuously changing sample (particulate and/or gaseous) - to minimize settling and/or mixing problems.

6. If consistent with other points, choice of a design which offers best development potential for pulsed laser use.

7. Linearity with pressure and independence of temperature.

On the basis of calculations and sensor and signal processing state of the art, the requirements could undoubtedly be met with a variety of designs based on the spectrophone concept. However, the desirable qualities appear to focus on the resonant spectrophone - with the exception of the last item. The significance of some of these listed points (1 through 6) has not always been well understood. These points will now be discussed in connection with specific designs.

It is fundamental from an S/N standpoint to obtain the information in the narrowest possible bandwidth. Absorption measurements could conceivably be dynamic in nature and require wide band response, but otherwise the passband width should be made to be very nearly zero.

Balanced Spectrophone

For the type of spectrophone with center frequency at approximately zero, near thermodynamic equilibrium exists within the sample cell. An extraneous signal which appears when this type of instrument is used results from interaction of the laser beam with the cell end windows. Absorption in the cell windows may be large with respect to the gaseous absorption of interest and is efficiently transferred into the medium. Since the time response of the system is too slow to avoid this effect,

the window signal is balanced out by using an identical series chamber with a gas of like thermal conductivity and with the same total pressure but without the absorber (Fig. 1) [10]. This "balancing" is delicate work and is sensitive to particles and imperfections on or in the windows. The very small absorption coefficients often measured in any of these cells result in correspondingly small temperature changes. As a result, the relative contribution to signal drift of external thermal sources or sinks acting through the cell wall can also become significant. Relatively long system equilibration times (generally 10 to 20 minutes) are thus required before measurements can be made. Even then, changes in external sources such as turn-on of electrical equipment, people in motion, cyclic air conditioning, etc., must always be considered. These problems can be minimized by insulation. The system must also be closed and isolated during the measurement. A relatively stabilized and temperature controlled version of a balanced spectrophone is discussed later in this report.

The pressure rise may be calculated for a given beam power and cross-sectional profile from consideration of heat conduction. The absorption coefficient can be calculated from the solution of the conduction equation:

$$\alpha(\text{cm}^{-1}) = 4\pi k \left(\frac{T}{p}\right) \frac{\delta p}{P} \qquad (5)$$

where k is the thermal diffusivity (watts/cm-°K), and p and T are the ambient pressure (torr) and temperature (°K); δp is the change in pressure (torr); P is laser beam power (watts); and B' is a dimensionless constant which depends on the laser beam radial intensity profile [4].

This type of spectrophone can thus be calibrated by using the above equation since all the quantities are either known or measurable. Another calibration technique involves the use of an internal calibrating source of thermal energy. However, to use this technique accurately the calibration source should have the same radial profile as that of the beam. This is simply not practical. The currently accepted approach involves the use of a well-known and verified absorption in either the gas of interest or one of nearly the same thermal conductivity.

Acoustic Spectrophone

Next to be considered is a device for which the passband can still be very narrow but whose center frequency is now in the audio range. The acoustical signals emanating from the volume of the laser beam may be generated by modulating this beam at the desired frequency. This frequency might, for example, be chosen to avoid 60 and 120 Hz line and high frequency amplifier noise. As was mentioned previously, the frequency

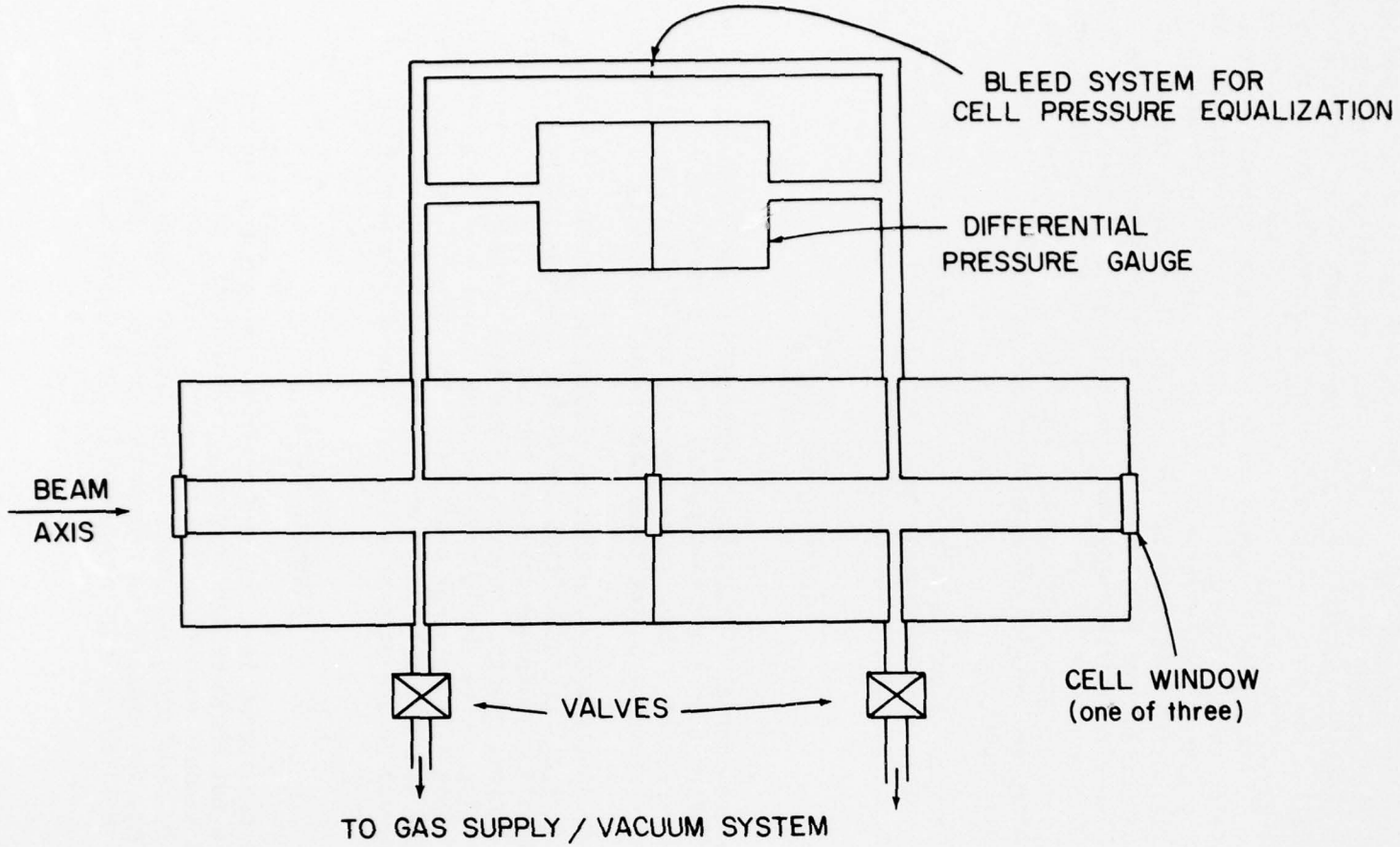

Figure 1. Schematic of differential spectrophone.

is limited by the time constant for the molecular relaxation to the translational state. This quantity is generally of the order of microseconds, though exceptions of much longer relaxation time constants (such as CO_2) are known.

For any given distance from the beam axis, an acoustical equilibrium will be established and a microphone can be used as a sensor. If the microphone is incorporated into an acoustically resonant chamber, an acoustical gain is realized. This gain is frequency selective and proportional to the Q value. The selectivity deriving from system Q is highly effective on a per-octave basis. Since filtering action is not flat in the passband, the modulation rate and the acoustical resonance must be mutually stable. The particular choice of Q value will be discussed in relation to the individual systems.

Resonances in cylindrical chambers have been discussed in detail in texts such as that of Morse [14]. Here the primary objectives in applying acoustical mode theory to system design were to examine dominant mode dependence on geometry, effect of driving force (pressure wave) symmetry on mode coupling, and nature of window signal coupling into the resonant chamber.

A chamber which may be approximated by a circular cylinder with perpendicular closed end walls has resonances at the frequencies

$$f = \frac{C}{2}\sqrt{\left(\frac{k}{L}\right)^2 + \left(\frac{\alpha_{\ell m}}{R}\right)^2} \qquad (6)$$

where L is the chamber length, C is the velocity of sound, and $\alpha_{\ell m}$ is the solution of $dJ(\pi\alpha\, r/R)/dr = 0$ at $r = R$, the radius of the cavity. This represents the condition that the particle radial velocity be zero at the cylinder wall. The k, ℓ, and m represent the longitudinal, azimuthal, and radial mode numbers. The resonant spectrophones of this report have been designed to emphasize either the longitudinal or the radial modes.

For coupling efficiency and for purity of acoustical mode structure, the resonant chambers of this report have been designed symmetrically with respect to the beam axis; i.e., they are made coaxial (excepting one experimental system). Another reason for this choice involves the possible occurrence of undesirable azimuthal acoustic mode dependence. This will be discussed under pulse source spectrophones.

The window signal has been represented as the problem child of spectrophones (resonant type spectrophones included). However, the cycle-to-cycle fixed phase relationship of driving frequency to resonance may be used

to separate the gaseous absorption signal from any window contribution. To accomplish this, the resonant chamber and internal microphone are formed into a subsystem (diagrammed in Fig. 2) which has apertures for beam entrance and exit but no windows. This subsystem is inserted into a larger system whose end windows are well removed from the apertures of the resonant subsystem. Any signals which are transferred from the windows into the gaseous medium at the driving frequency are first dispersed. The surviving window signal is then mismatched to the resonant chamber so that the contribution to the gaseous absorption signal is negligible. A phase selective signal processing system utilizing a lock-in amplifier reinforces this filtering electrically. This option is an essential aspect of the measurement system and is largely responsible for the primary choice of an acoustically resonant system. Physical simplicity is achieved without compromise while requiring elegant but commercially available electronics. The use of the phase of the signal ensures that the maximum information content is extracted from the signal. Another way of appraising the advantage of the audio frequency, phase-locked system is to consider the effect of the use of phase on bandwidth. Phase locking, when overtones are excluded, is equivalent to reducing bandwidth to virtually zero; i.e., if one phase locks to a fixed frequency source for endless time, the bandwidth would be zero. For the absorption measurements contemplated, the effect of signal amplitude changes on the frequency is negligible.

The phase selectivity also allows suppression of other potentially noisy operational modes, such as pumping sample gases through the system while taking data. The noise created by flowing air generally does not contribute to the phase locked signal (unless pulsations are strong) though dynamic overload may become signficant. These facts can be of great use and illustrate that such a system does not require acoustic isolation and can be applied to absorption measurements systems without acoustical isolation. Furthermore, it should be pointed out that thermal isolation is totally unnecessary since there is no particular sensitivity to this. Mechanical vibrations are also phase selected out. When approaching the sensitivity limit, some of these perturbations might appear on the signal, at least, to a small degree. To date such signals have been within the noise, though noise levels are typically 20 to 30 nv.

Calibration as an absolute sensor is not presently a satisfactory option for resonant systems. In fact, it would be very difficult to attain an absolute calibration having the accuracy obtainable using well-known absorption coefficients to normalize one or more relative quantities of a set. For resonant spectrophones, the quantities which are ingredients of such an absolute calibration are difficult to measure or calculate with high accuracy. For example, the acoustical mode structure will not be simple for the length to radius ratios used (L/R not >>1). Calibration of the interaction between acoustic wave and microphone diaphragm adds another

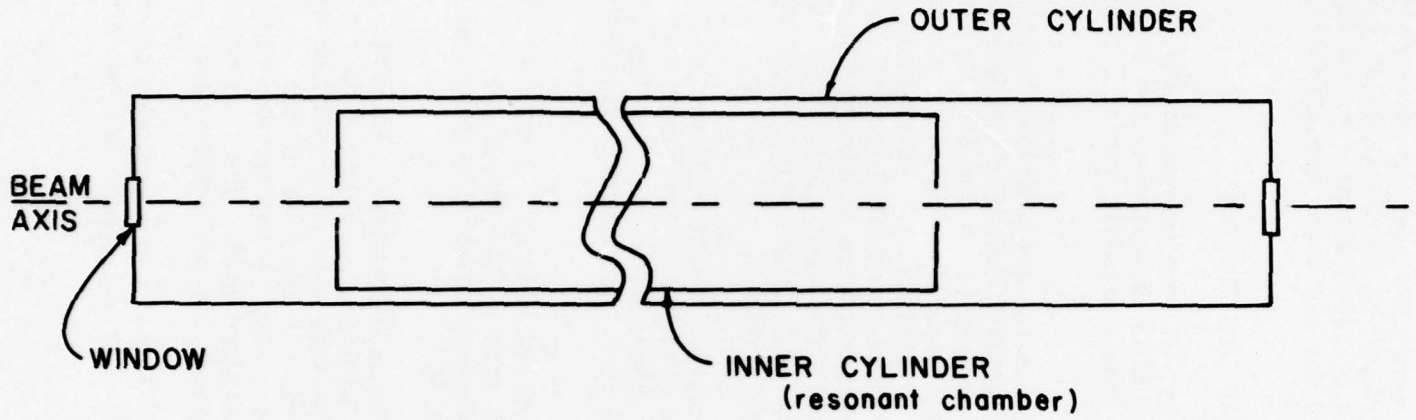

Figure 2. Schematic of resonant acoustical spectrophone.

degree of complexity. It must also be noted that the net quantity cannot be assumed to be linear, with system temperature and pressure. However, since all of the systems of this report are used to investigate absorption by atmospheric gases, usually broadened as naturally by an N_2/O_2, 80%/20% buffer, only one parametric matrix of calibrations for the range of temperatures/pressures is required for all trace contaminants.

MICROPHONE CONSTRUCTION

Each capacitance microphone consists of an aluminum coated, mylar diaphragm. To give resilience and high capacitance, the diaphragm is spaced periodically and minutely from a metallic surface. The surfaces are either planar or cylindrical.

The thickness of the mylar depends on the application. For higher sensitivity, higher microphone polarizing potentials and/or thinner diaphragms with greater displacement responses for a given pressure variation are employed. The capacitance also increases for thinner diaphragms, further increasing the sensitivity. Thicknesses of 0.002, 0.001, and 0.0005 inch are used though standard thickness is the 0.002-inch value. This thickness gives good sensitivity together with negligible mechanical hysteresis. In the small diameter, cylindrical chambers most often used here, the 0.002-inch mylar is also largely self-supporting by virtue of its own monocoque resilience.

The spacing mechanism varies and may either be machined in the rigid metallic supporting surface or be attached to the mylar - in the form of narrow mylar strips with separations which optimize the sensitivity. Typical spacing is 0.003 to 0.015 inch with spacer separation from 0.25 to 0.5 inch.

The mylar is aluminized by evaporative coating. A mask is used so that the coating does not approach the edge of the diaphragm. This prevents arcing across the gap by the microphone polarizing potential which is generally between 100 and 1000 volts.

Figure 3 shows an example of a planar microphone. The Fig. 3 insert shows an end-on view of the same microphone illustrating the machined-in form of the metallic spacers. The same type of microphone has been constructed by using mylar spacers. In the case of Fig. 3, the diaphragm is supported by a brass plate which also serves the function of making contact with the diaphragm's aluminized side. The beam entrance to this (experimental) system is through the off center port.

Figure 4 shows other diaphragms. These do not yet have spacers mounted. The circular ones are for the end-wall microphone and the others are

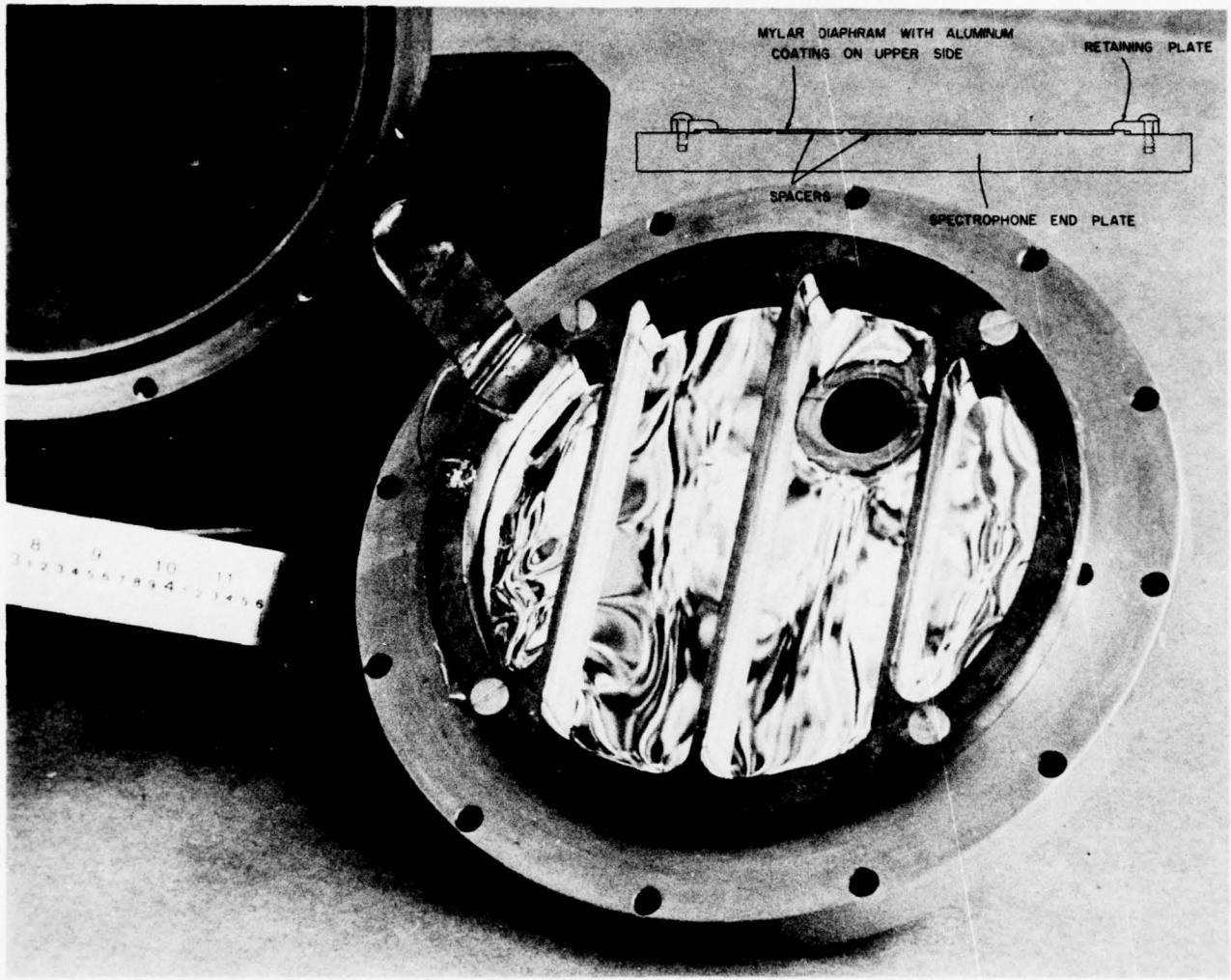

Figure 3. End-wall microphone.

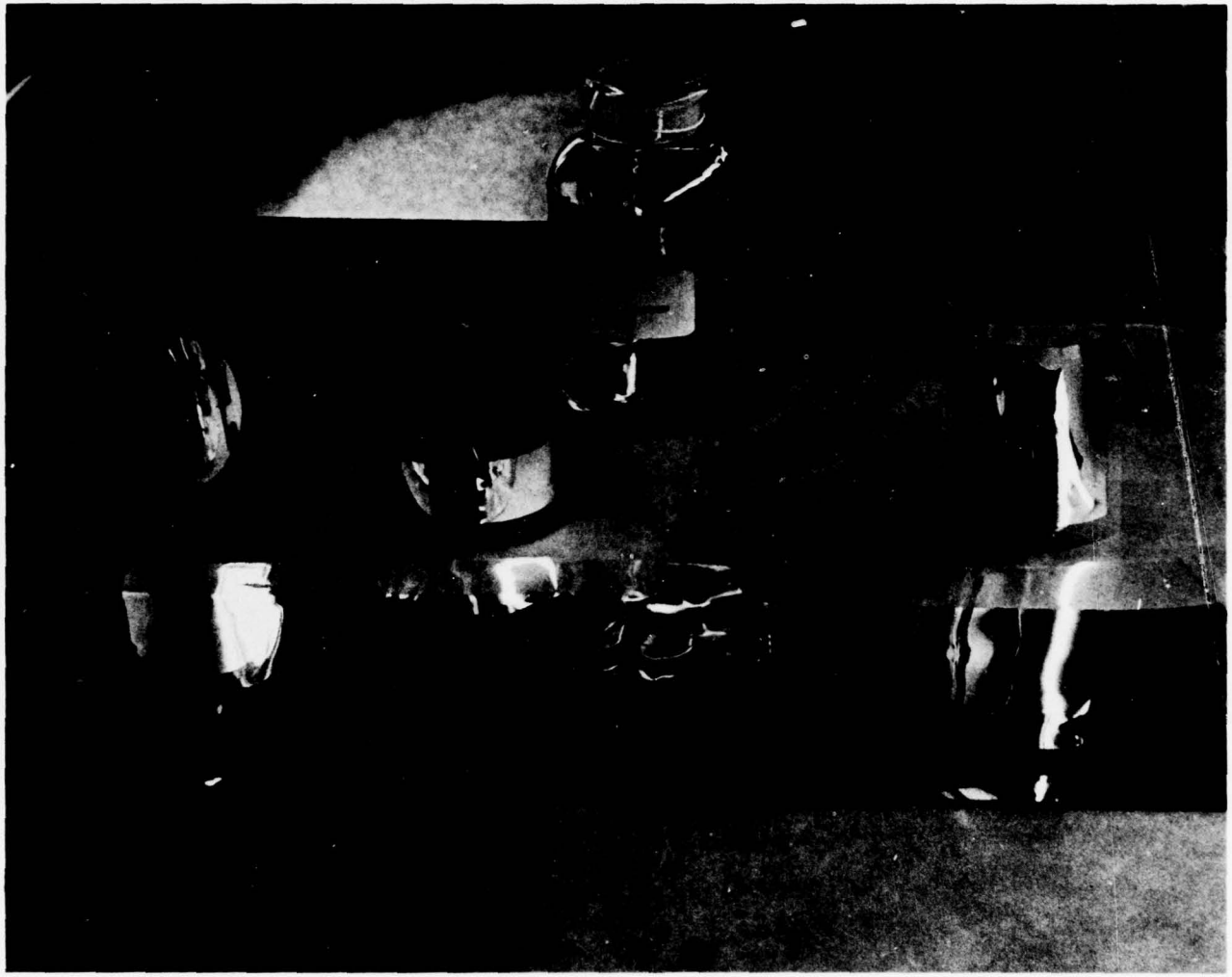

Figure 4. Microphone diaphragms - unmounted.

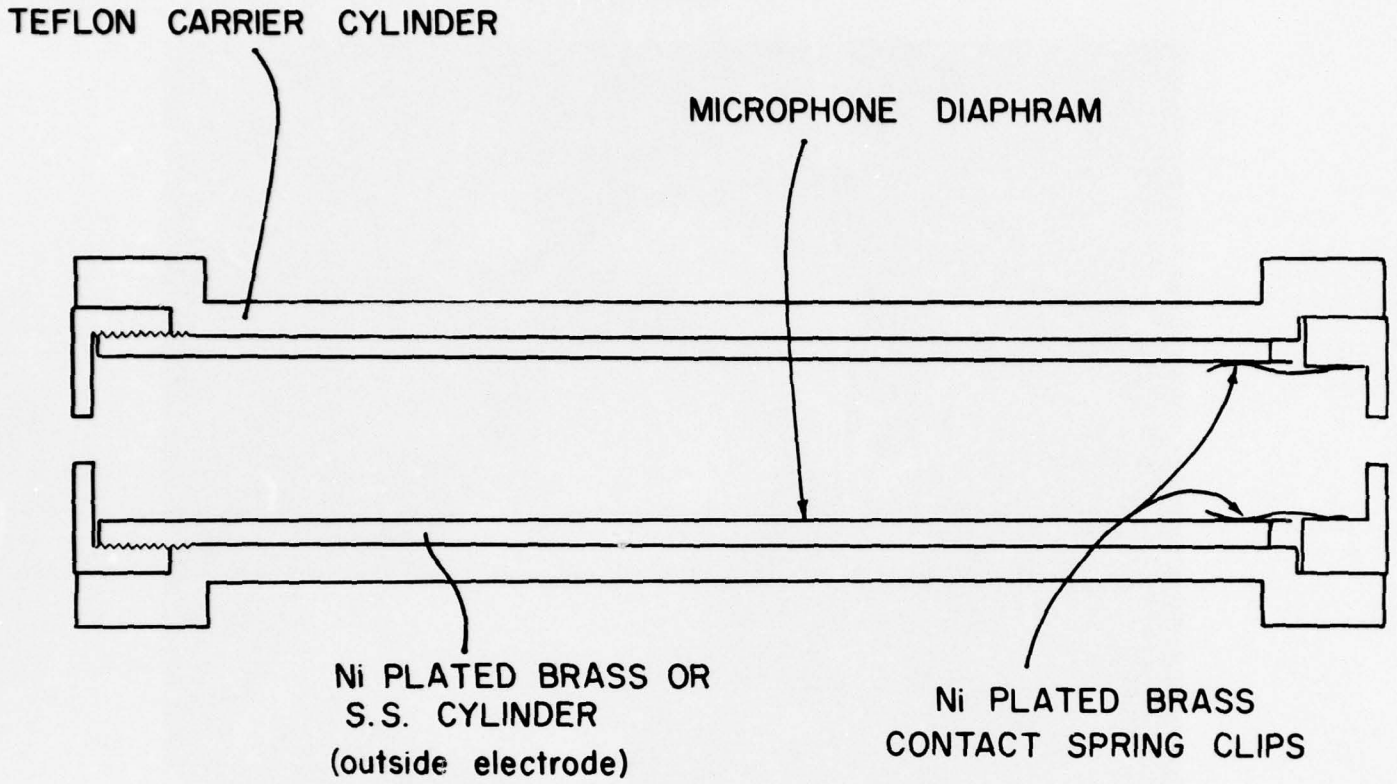

Figure 5a. Drawing of components of cylindrical microphone.

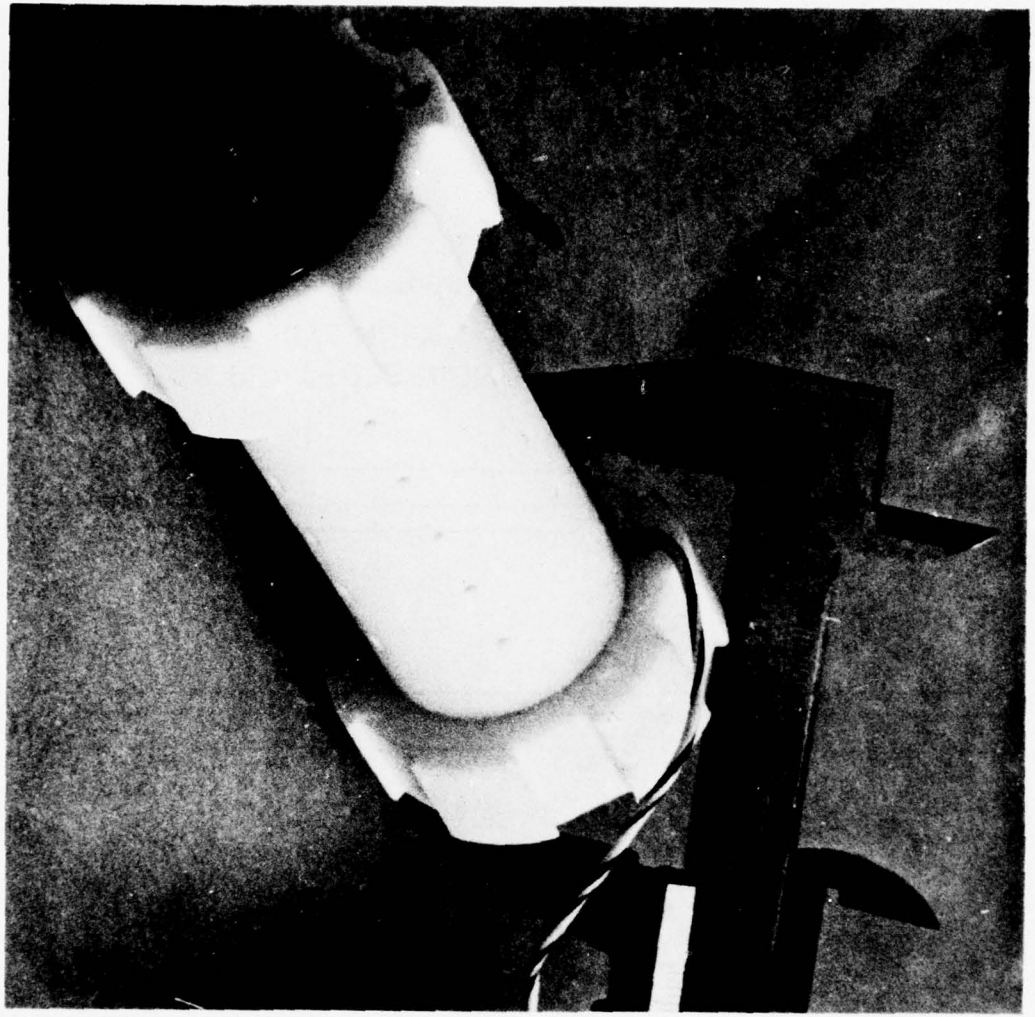

Figure 5b. Photograph of cylindrical microphone.

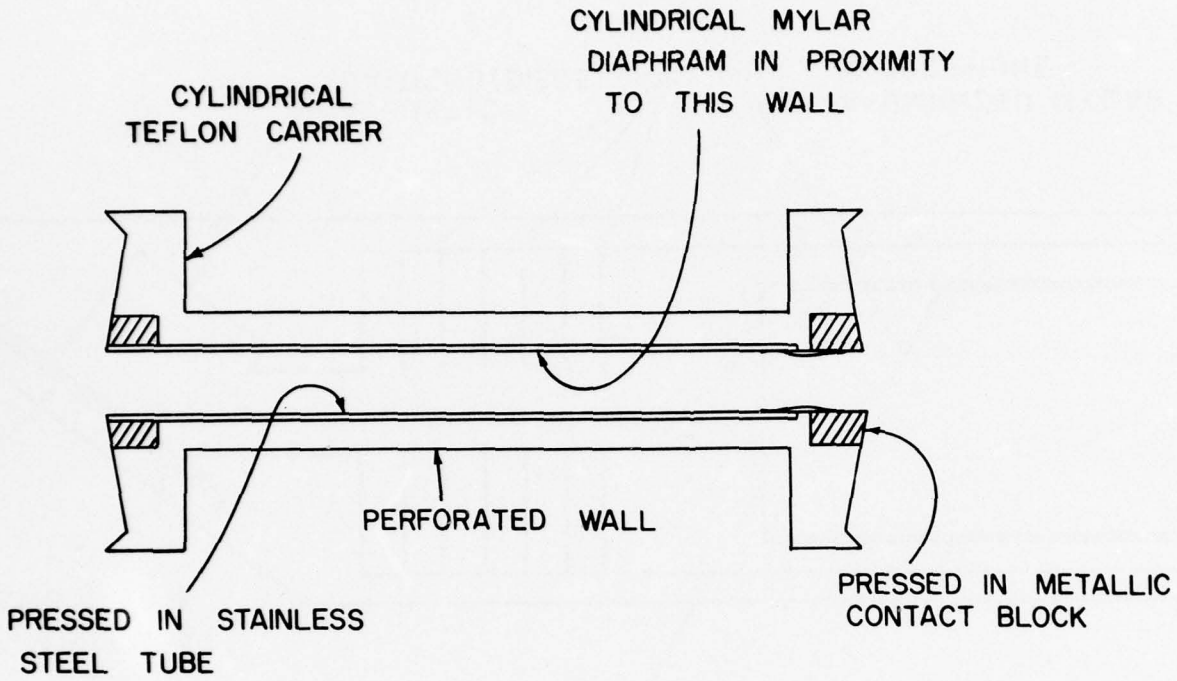

Figure 6. Double open ended organ pipe type of resonant microphone.

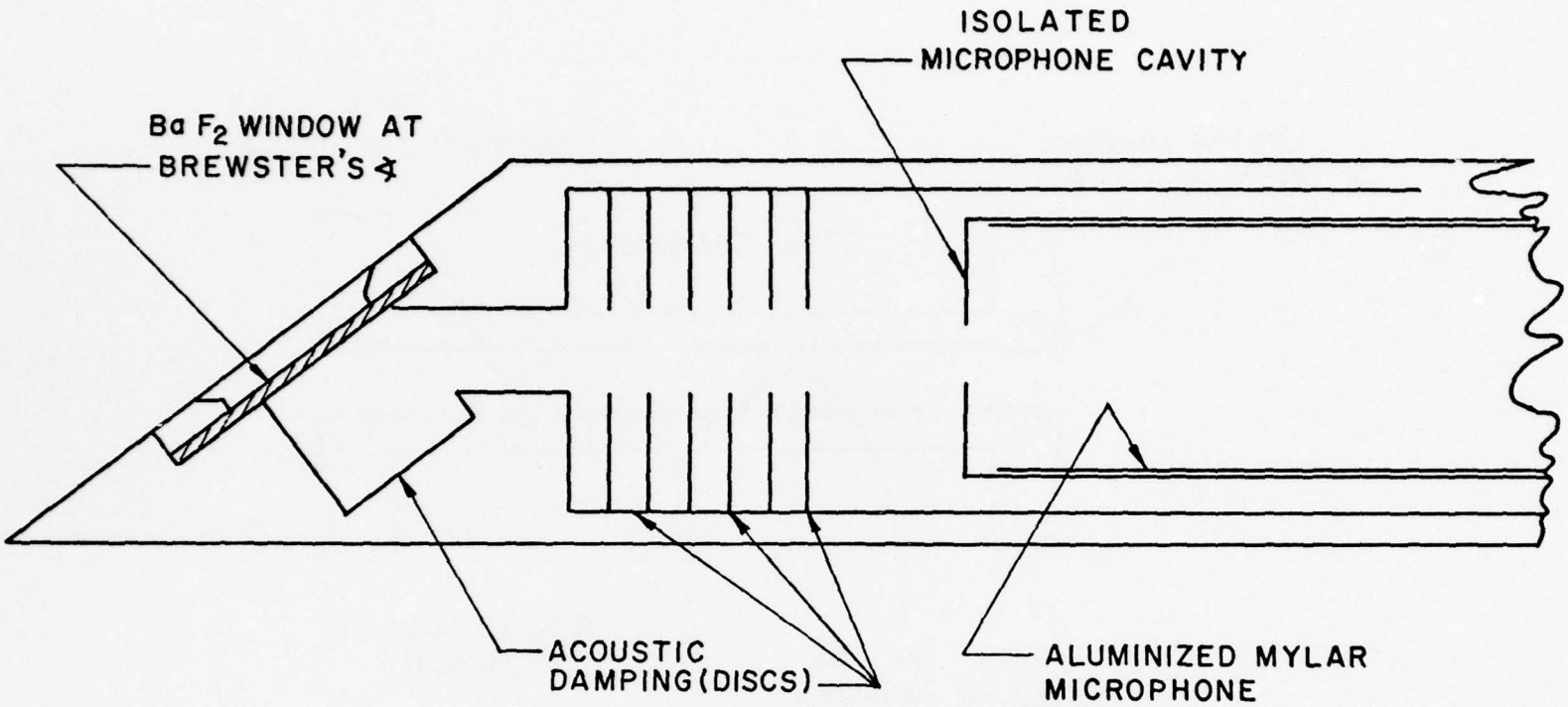

Figure 7. General-purpose CW source spectrophone.

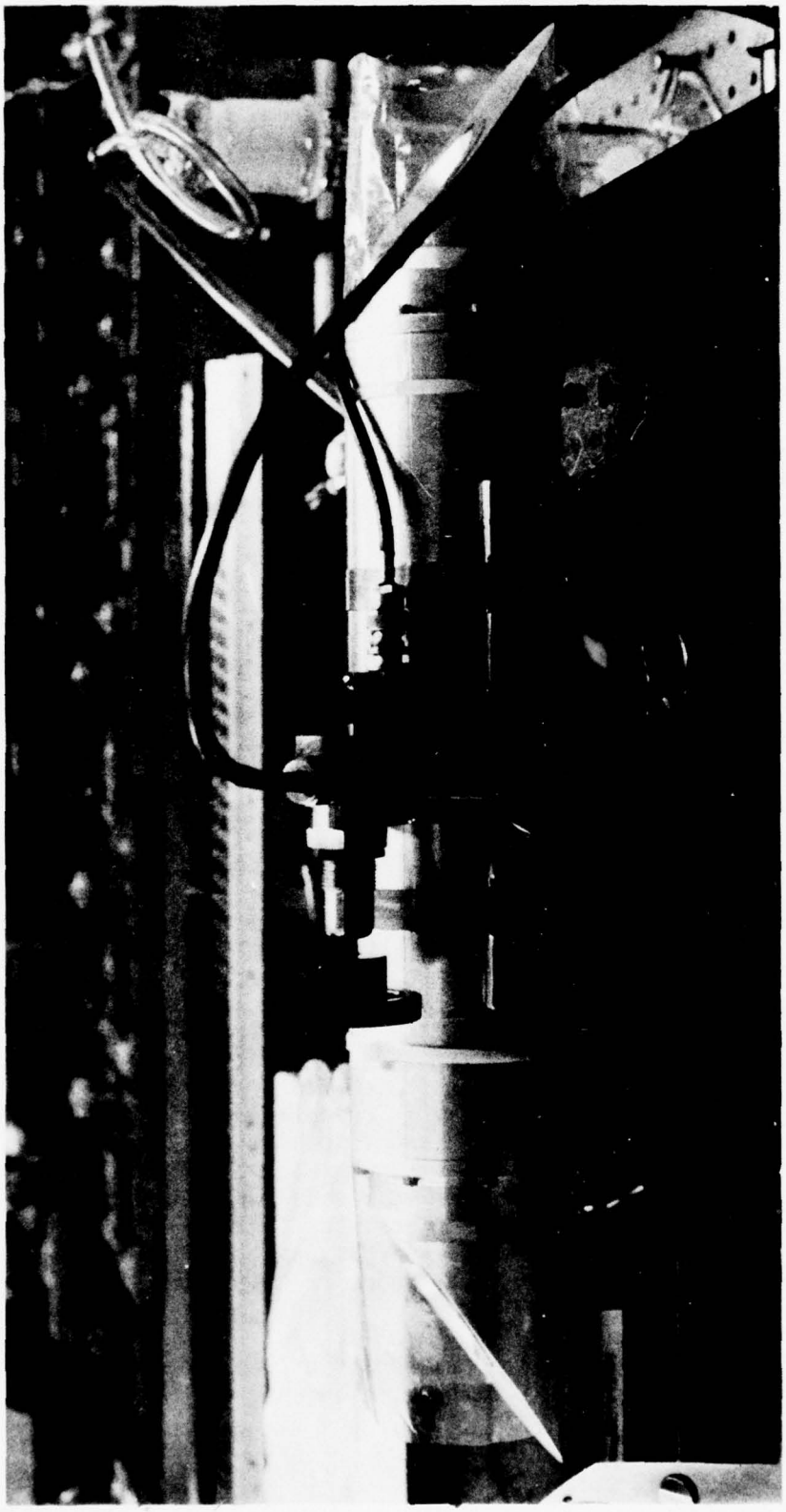

Figure 8. CW source spectrophone.

dimensioned for specific cylindrical microphone sizes. Of the approximately dozen cylindrical microphones used, there are four different diameters, three of which are pictured. The remaining microphone is much larger, i.e., approximately 7 by 25 inches.

The cylindrical chambers are generally constructed of nickel plated brass or stainless steel within a teflon mount, giving both acoustical and electrical isolation. Nickel plating of the brass reduces surface deterioration. Without describing obvious mechanical details, Figs. 5a and 5b show the components of a typical system. The inner diameter is 1-3/8 inches. Note that the cylinder is relieved at frequent spatial intervals. This prevents microphone damage during pumping and ensures that the resilience is due to the mylar.

Another microphone is a double open-ended organ pipe (Fig. 6) as opposed to the double, semiclosed type. This small bore system is closely matched to the beam diameter and has a fairly pure longitudinal mode structure.

Resonances within the diaphragms themselves have been studied by using acoustic sources and acoustically spoiled chambers. The spectral results are not smooth but reveal no peakiness of concern for the resonant frequencies of the chambers.

SPECIFIC CW-SOURCE SYSTEMS

General-Purpose CW-Source Resonant Spectrophone

The first spectrophone to be described is simplest and yet has a broad range of applications. Figure 7 is a sketch of a spectrophone which illustrates the essential simplicity of the design. A photograph of the same cell follows as Fig. 8. The focus is on the acoustically isolated microphone chamber within the larger spectrophone cell. The resonance as discussed previously occurs within this inner chamber. It will be noted that the windows are located only at the ends of the outer chamber. The housing material first used for these spectrophones was aluminum; however, type 304 stainless steel is preferred because it improves system purity and stability by reducing porosity and interaction with absorbers. Microphones of 1/2 and 1 inch as well as the usual 1-3/8 inches inner diameter have been inserted into absorption cells such as the one illustrated. Preferred resonant chamber length is 8 inches, giving a principal resonance at about 1 kHz (STP). One coaxially shielded electrical lead and one vacuum/gas input connection only are required for operation of the spectrophone. Temperature sensors are attached to the cell outer wall.

This spectrophone will now be discussed as applied to general gaseous absorption measurements at CO_2 laser wavelengths.

Figure 9 is a schematic of the entire optical system. The laser is a stabilized, line tuneable unit (Sylvania Model 950) whose single-line power output ranged from about 0.5 to 3 watts for the lines employed. A colinear HeNe laser is used to monitor alignment. Two detection systems are shown: one is a power meter and the second is a time resolved detector for tuning the spectrophone and observation of the synchronized component. This latter technique is a visual phase selective system and is simply qualitatively informative.

Finally, an IR spectrograph using a U-V pumped, calibrated fluorescent analyzer plate at the output plane allows continuous monitoring of the wavelength output of the CO_2 laser.

Figure 10 shows signal processing for the same system. As has been discussed, this is an essential part of the measurement system. The choice of a phase selective system partly reflects the fact that it is fundamental from an S/N point of view to obtain the information in the narrowest possible bandwidth. Passband location is always chosen so as to avoid line noise as much as possible. Records were made directly on chart paper by two ways. First, and most generally, spectrophone signal amplitude was plotted against time. A measurement cycle is as follows. A solenoid driven paddle blocks the CO_2 laser beam while a baseline is established. When the beam is unblocked, the spectrophone signal stabilizes at the absorption signal level. The stabilization time is determined by the integration time constant of the lock-in amplifier. This unblocked status is generally sustained for several minutes to check any tendency for drift. Then the beam is again blocked to recheck the baseline. Figure 11 is a sample signal form which represents the modulation - not the carrier.

X-y recorder plots of signal versus power, another form of presentation, are important as tests of system linearity and are performed occasionally. Figure 12 shows one of these plots. Decreasing the laser pump power to threshold results in the cutoff. An attenuating optical element can then be inserted in the beam and the curve continued to lower levels.

Compilations based on data accumulated over an extended period are then compared for reproducibility and pattern agreement with the most significant previous results (generally obtained using a White cell). Finally, the relative spectrophone signals are normalized to those of the White cell results. Examples of the results of this process are presented in a following section.

Vacuum/Gas Handling System

The vacuum/gas handling system is an important external element in these measurements because of its part is assuring spectrophone and gas purity. The system to be described here (diagrammed in Fig. 13) performs several

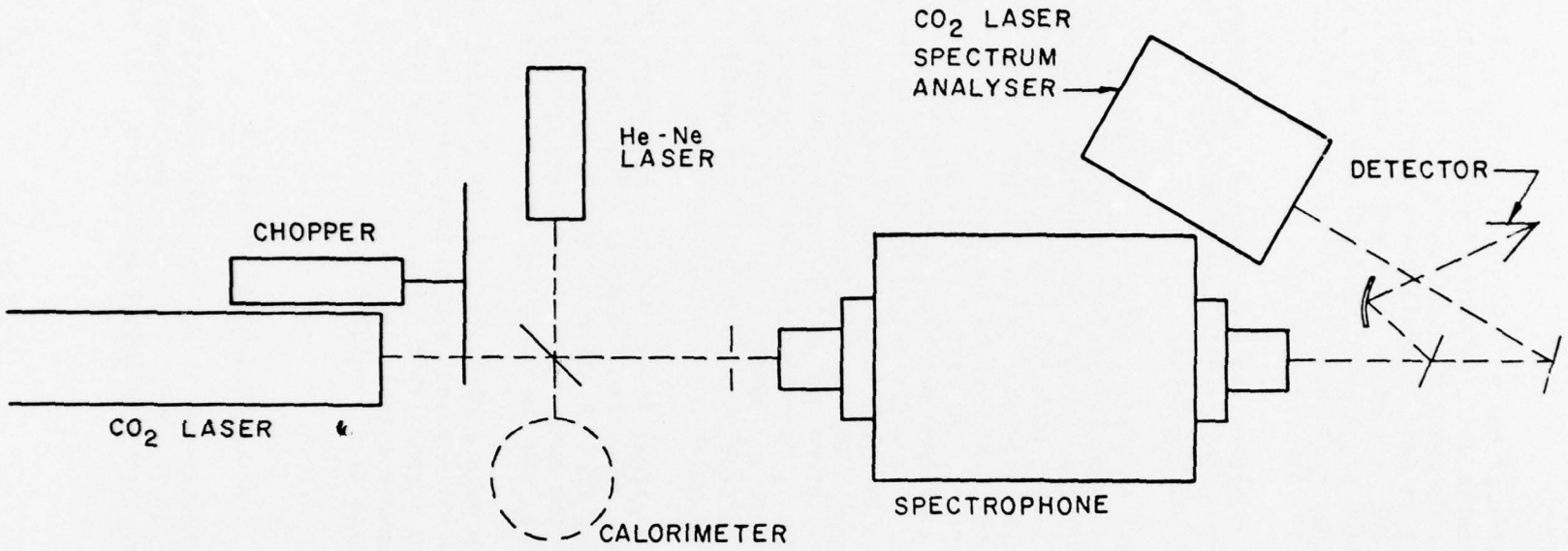

Figure 9. CW source spectrophone optical system.

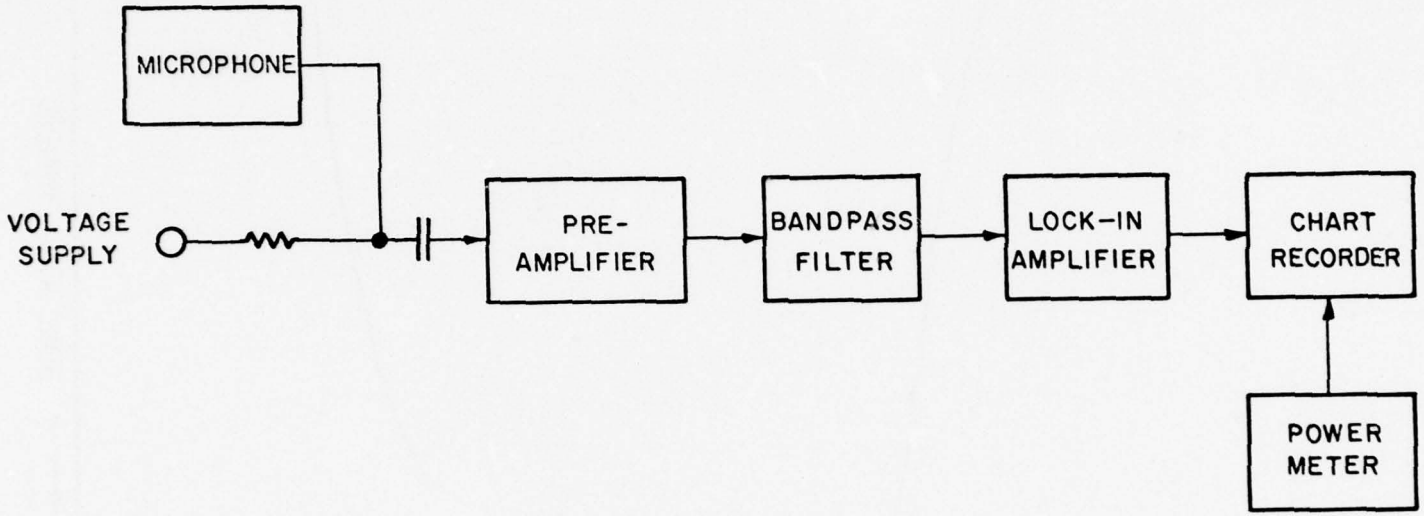

Figure 10. Signal processing for the CW source spectrophone.

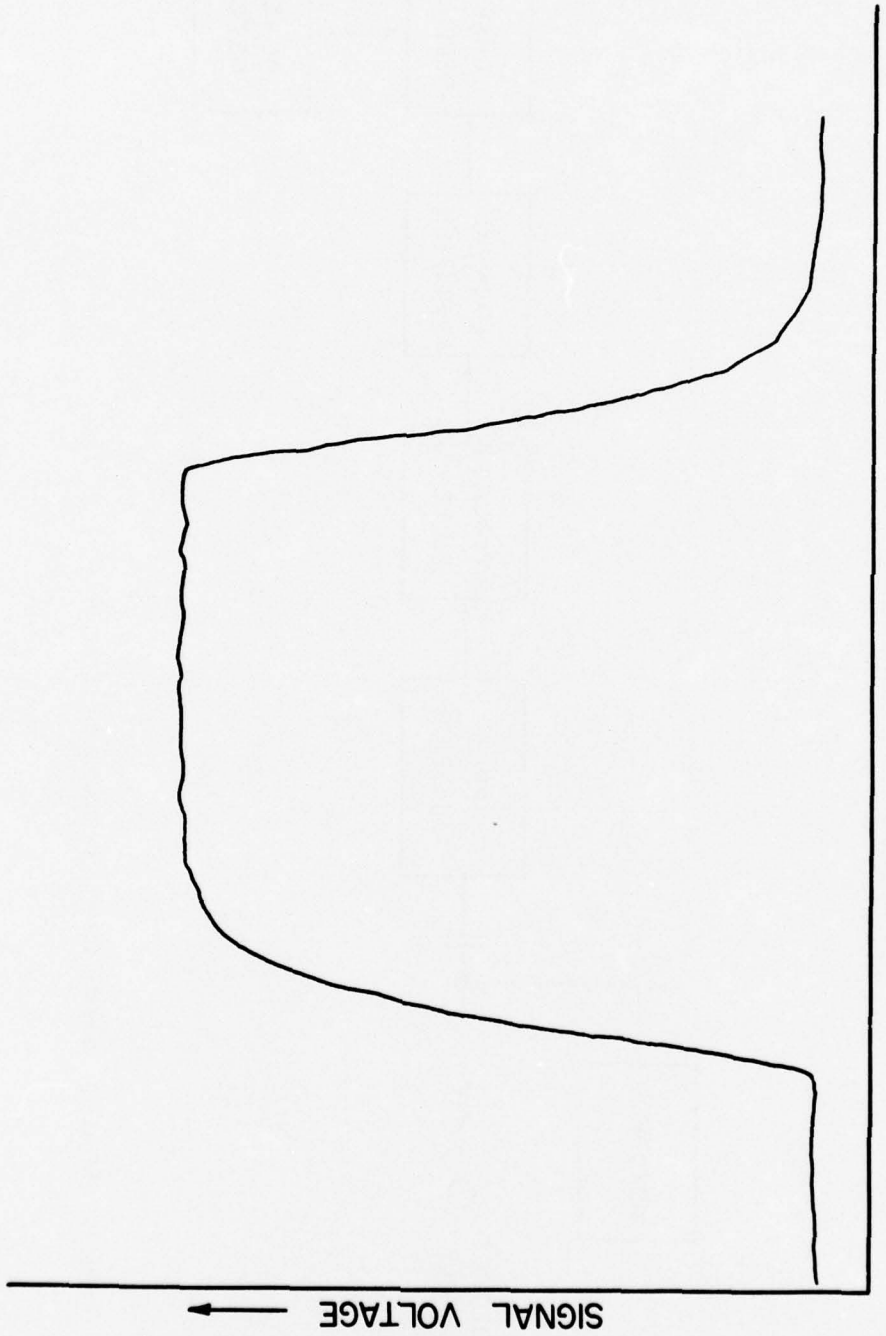

Figure 11. Sample signal: relative absorption vs time.

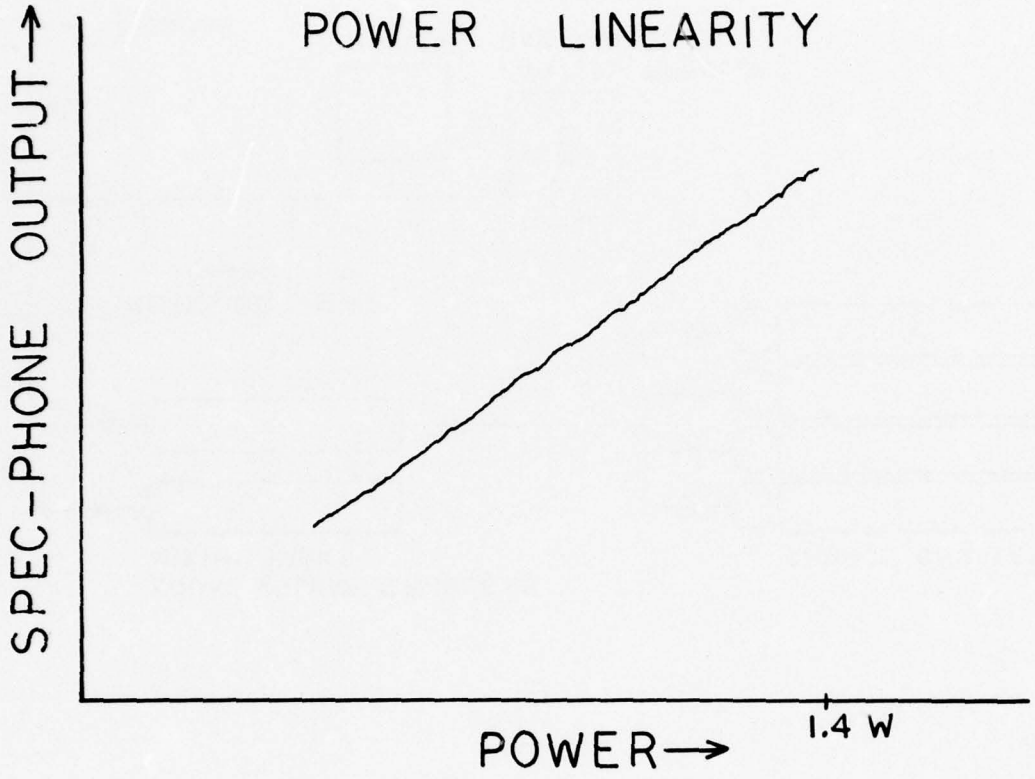

Figure 12. Sample signal: power vs relative absorption.

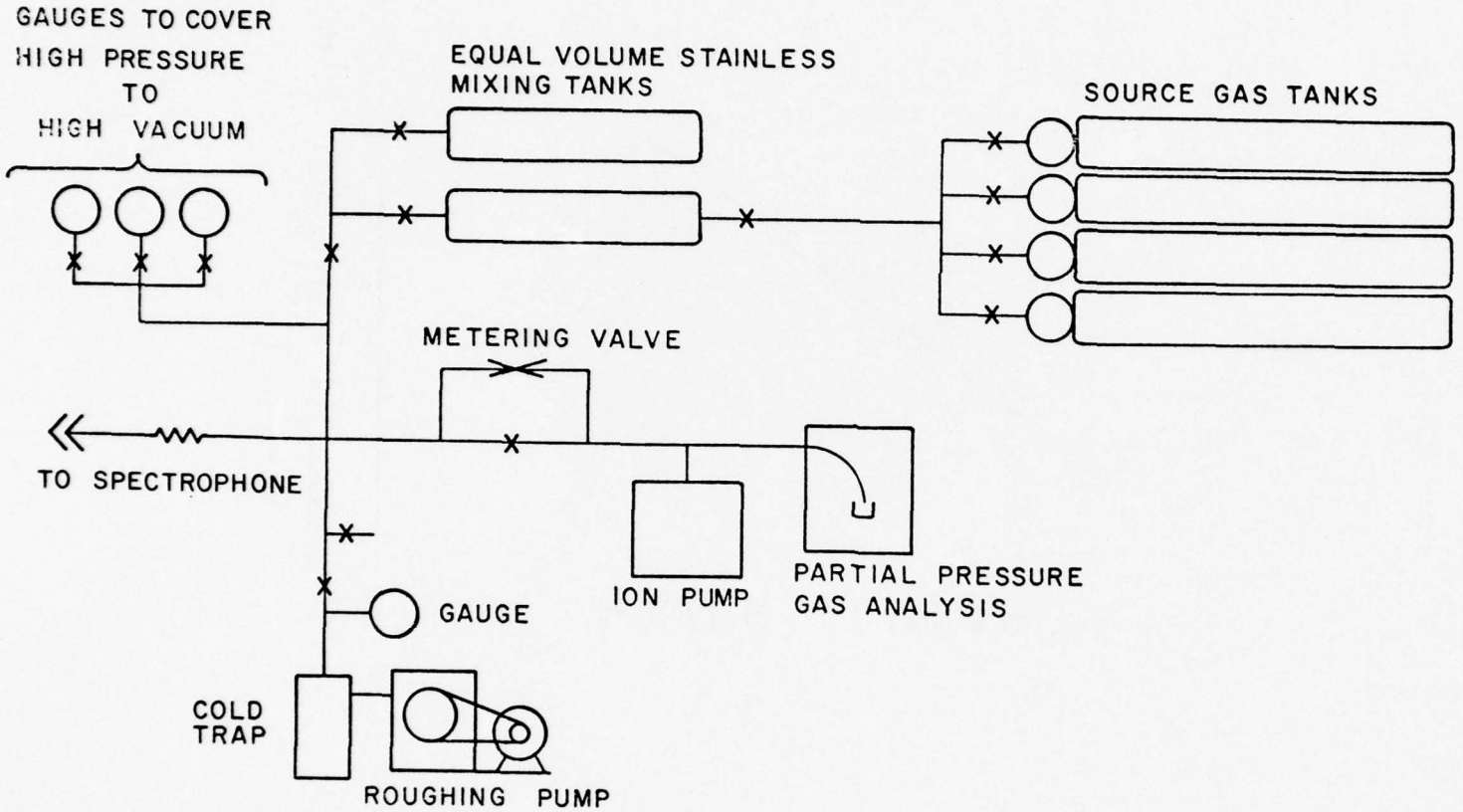

Figure 13. Schematic of vacuum/gas handling system.

essential functions without requiring disconnections. First, it serves as a high vacuum pumping station during the bakeout cycles. It is then used for mixing the high purity gases. Note that this two-tank design, with gauges ranging from high vacuum to high pressure, allows mixing of any number of gases in desired proportions. The volumes of the two tanks with valves were made essentially equal and thus calculation of the ratios of gas partial pressures is simplified. Total and partial pressures of desired constituents and impurities in the cell are monitored with system gauges and a mass spectrometer gas analyzer.

Figures 14 and 15 show the arrangement of the elements. The entire system is on wheels and connects to gas tanks and spectrophones by stainless steel flexible bellows (high vacuum) lines.

CW-Source Cooled Resonant Spectrophone

The next system to be described is based on the same physical design as that of Fig. 7 but includes a thermal reservoir for the stabilization of absorption cell at temperatures well above and below laboratory values. Figure 16 shows the essential features of this system. The reservoir tank is heliarced around the spectrophone and this entire unit, with the exception of the spectrophone chamber ends, is surrounded by styrofoam and encased in a wooden housing. Another newly introduced element is an antifrost system for the absorption cell end windows, including a second vacuum system. In essence, the inner windows are isolated from moisture and the outer ones are isolated from the low temperatures by use of the phenolic spacer tubes at each end of the spectrophone. This system proved to be quite adequate. Two spectrophones (Figs. 17 and 18) of this type have been used to measure absorption of CO_2 laser radiation at STP and 210°K and lower pressures. For this purpose, a U-V lamp with quartz envelope produces an ozone equilibrium in the cell. The quartz envelope of the lamp is an internal fixture of the system and preserves the spectrophone high vacuum integrity and bakeability.

When used for measurements at low temperatures, the reservoir tank is filled with ethyl alcohol, and chunks of dry ice are used to obtain the desired temperature. Once in equilibrium, the spectrophone temperature drift is very slow (about 3C°/hr at -60°C), allowing a complete set of measurements at the desired temperature.

Figure 19 shows the pattern agreement with previously obtained White cell results for the only conditions for which the reference (White cell) values were obtained. Speaking generally, relative comparisons between independent IR absorption measurements are rarely this close.

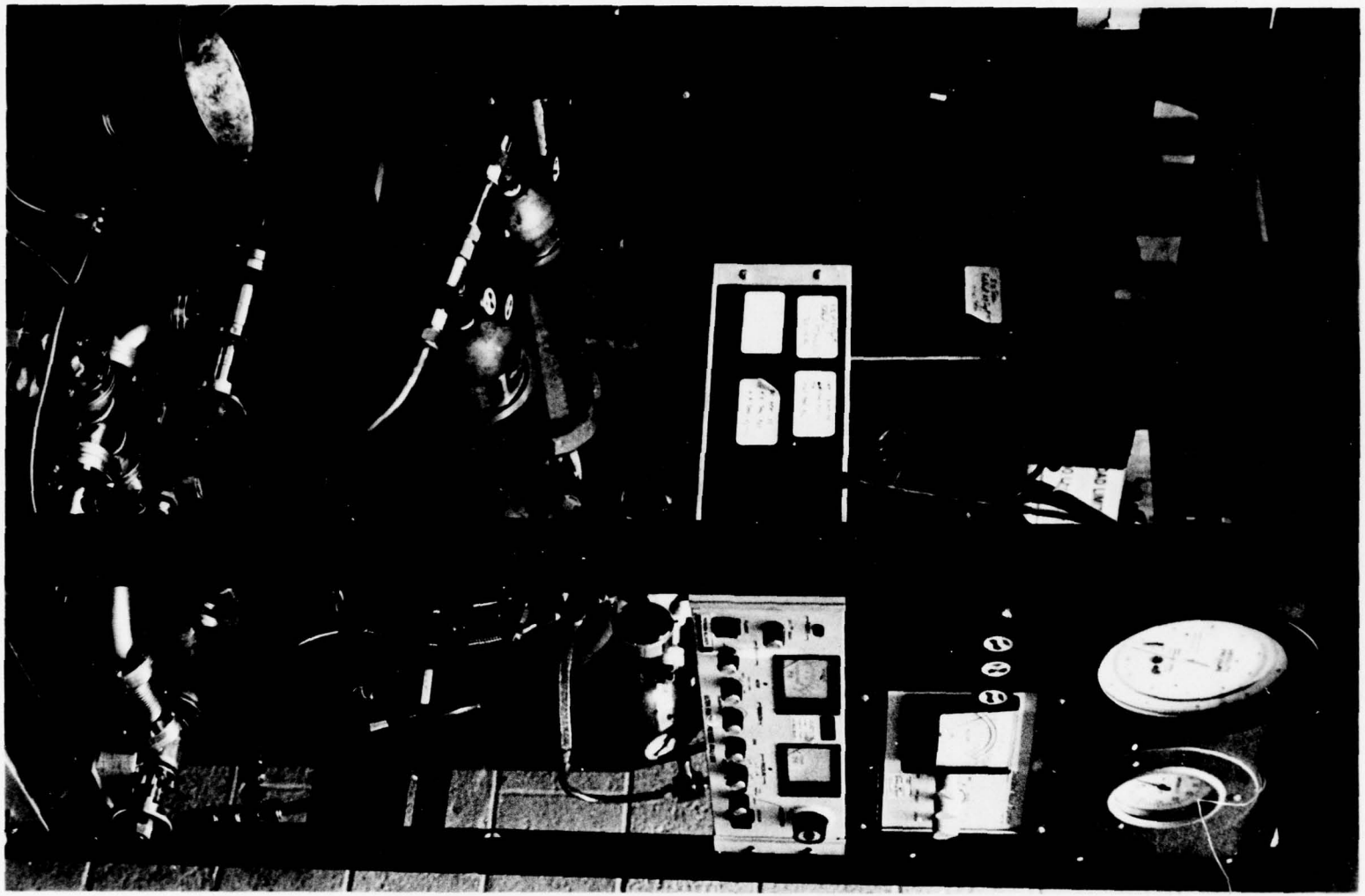

Figure 14. Portable gas handling system.

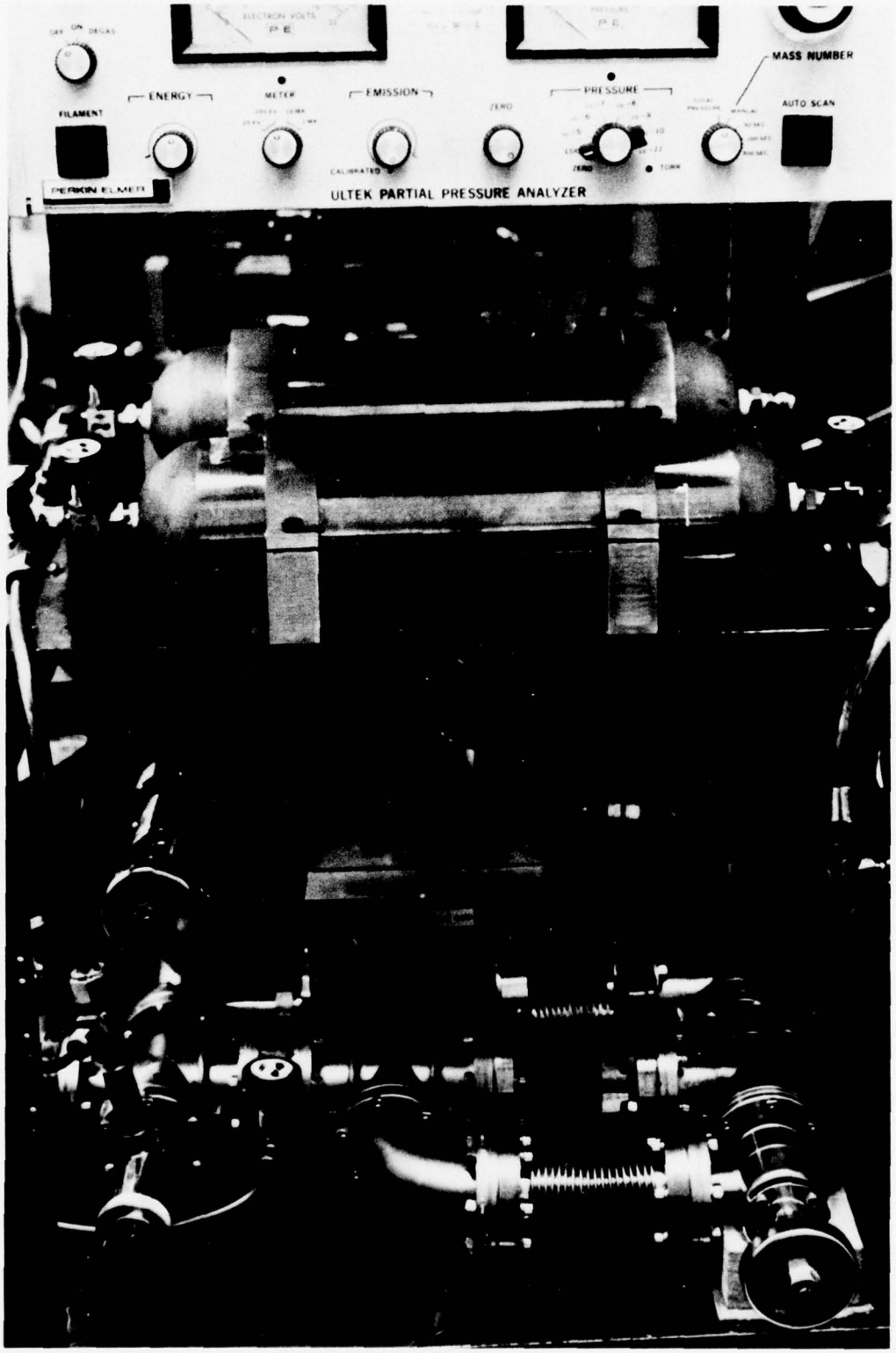

Figure 15. High vacuum portion of gas handling system showing mass spectrometer gas analyzer.

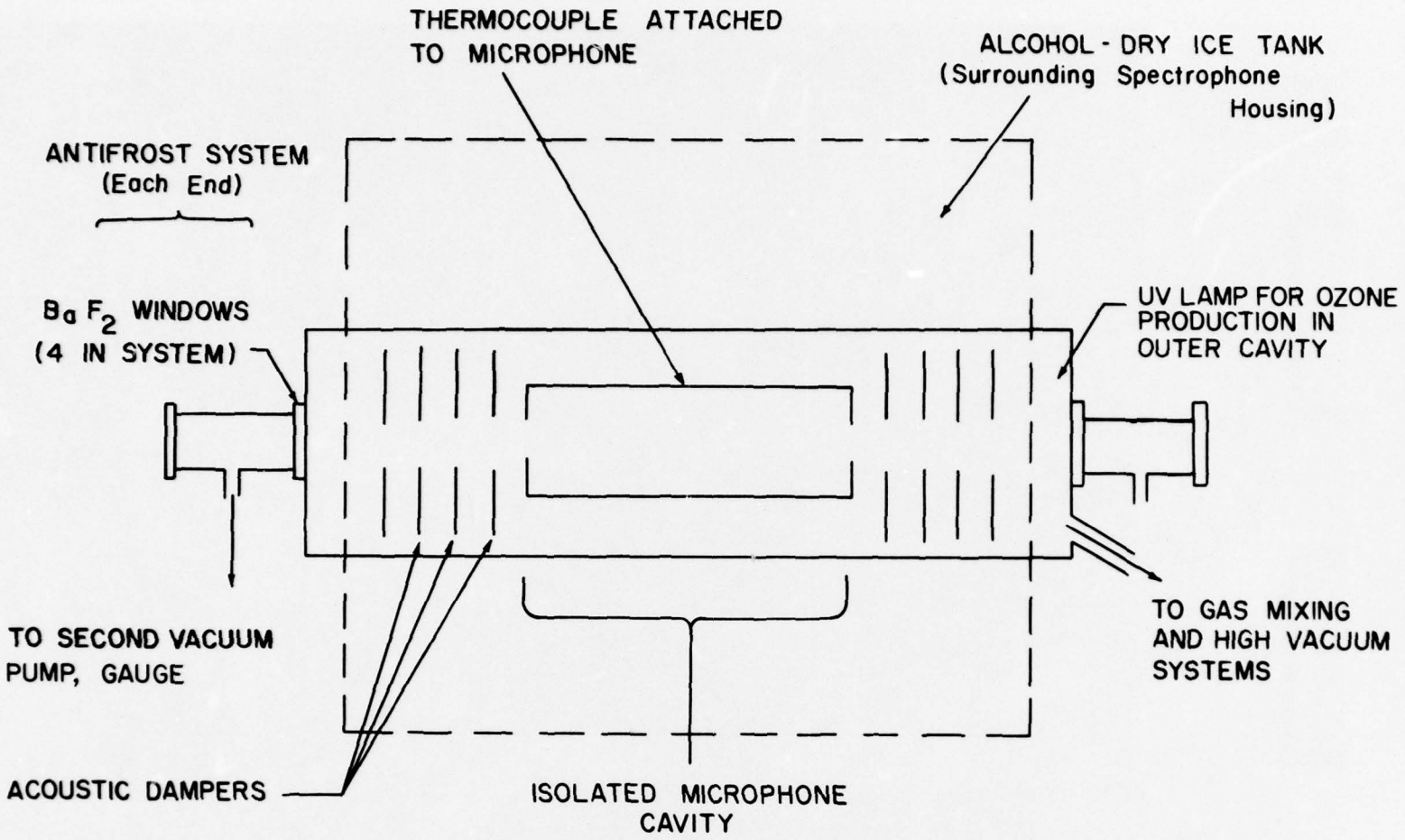

Figure 16. Schematic diagram of temperature controlled CW source spectrophone.

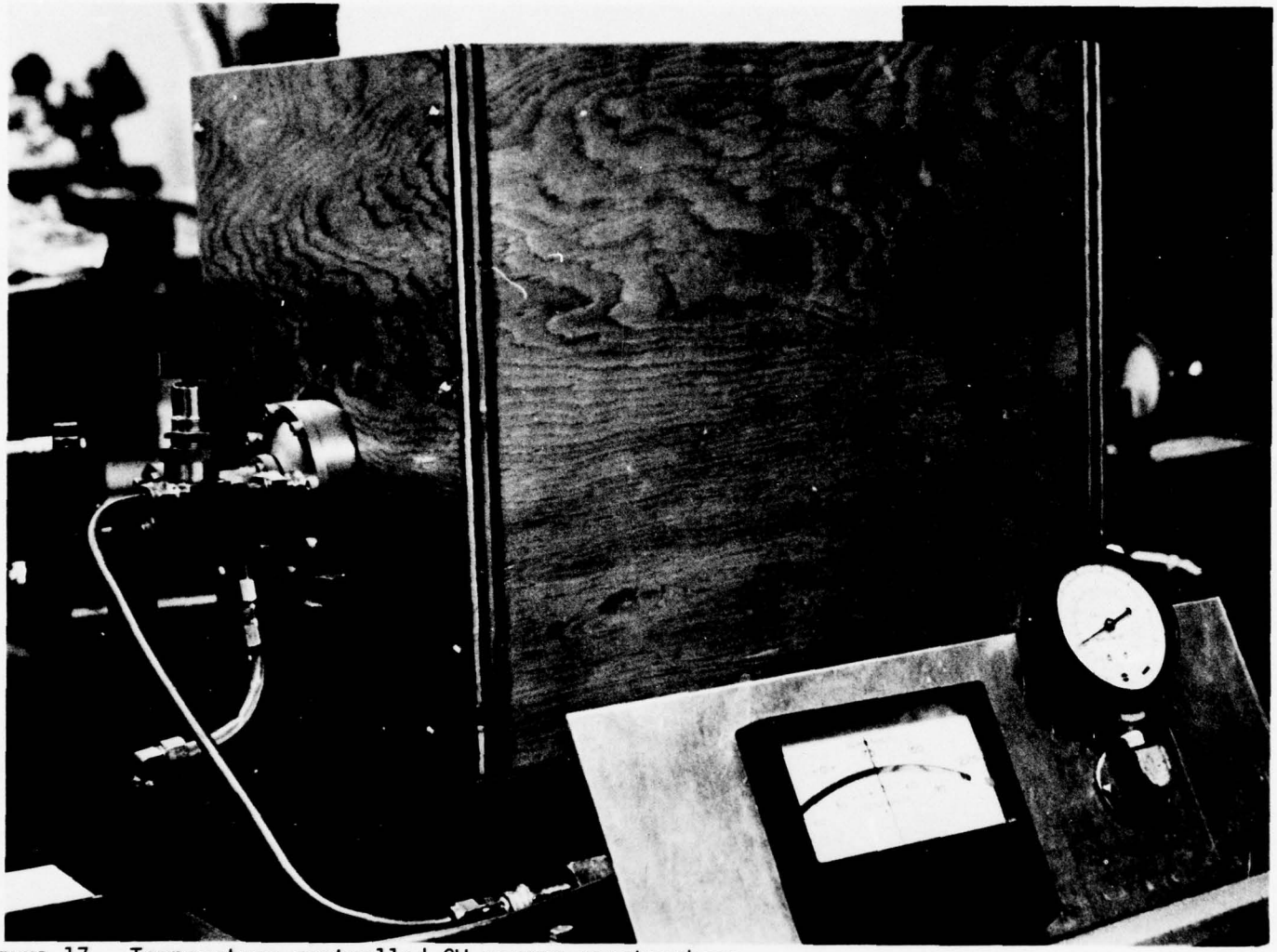

Figure 17. Temperature controlled CW source spectrophone.

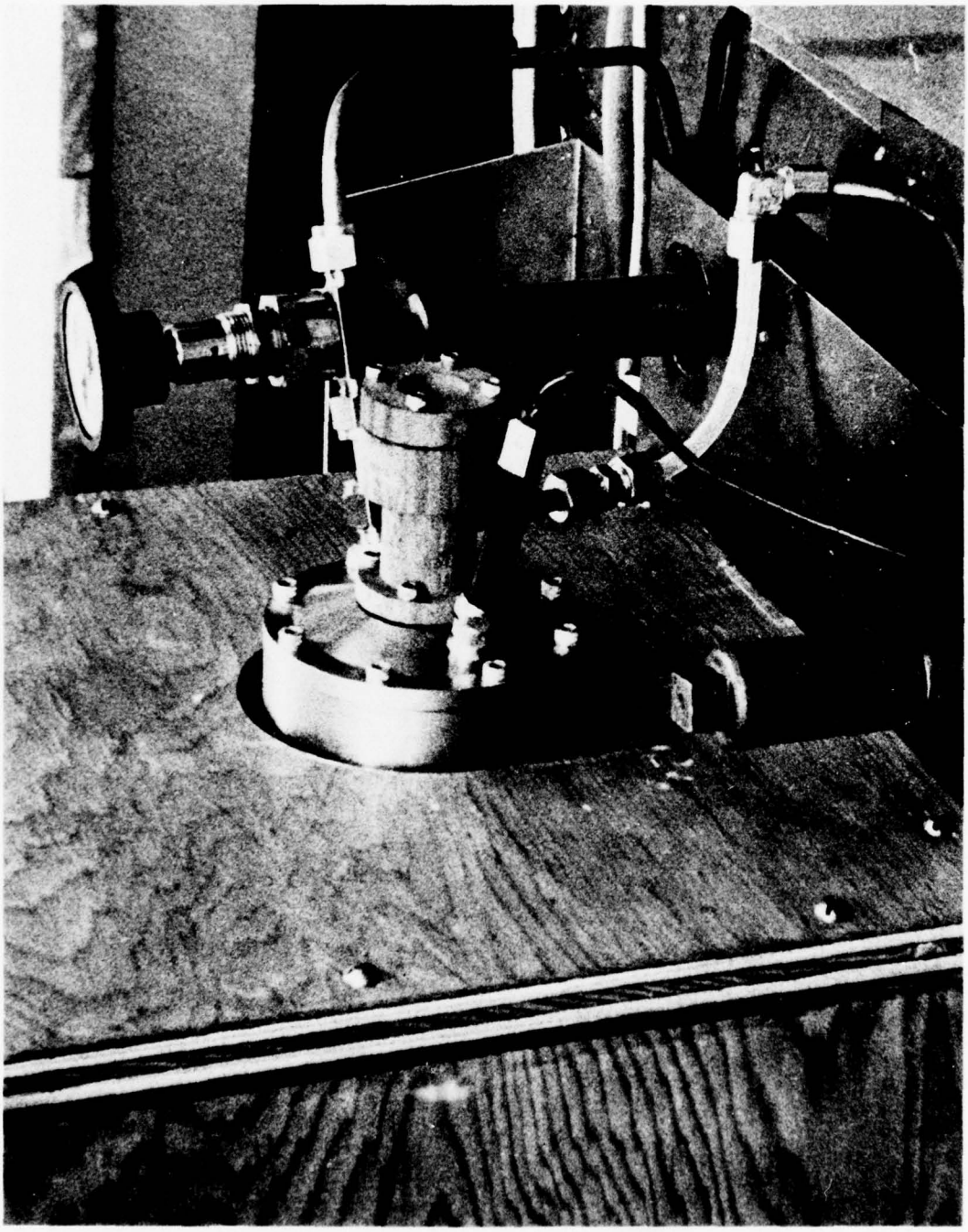

Figure 18. Temperature controlled CW source spectrophone.

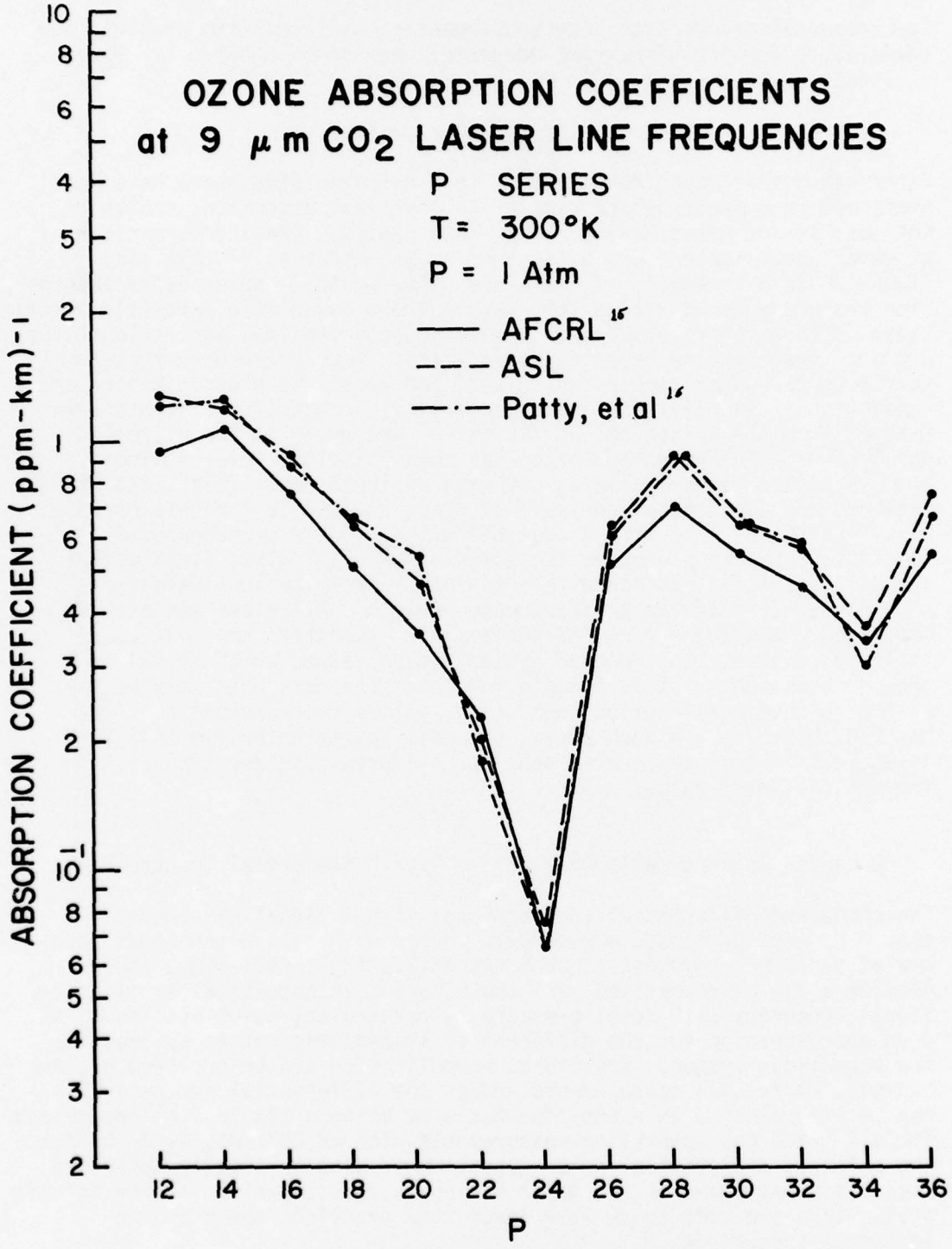

Figure 19. Pattern comparison for spectrophone and White cell absorption measurements. Ozone absorption coefficient is plotted vs laser line. The line connections between points are for visual ease of identification only.

Spectrophone measurements were subsequently continued into pressure and temperature domains either not adequately performed previously or non-existent.

CW-Source Water Vapor Measurements

Water vapor absorption measurements in a nitrogen atmosphere have been performed in a spectrophone similar to that just described, though in this use it was often heated rather than cooled. Continuous monitoring of water vapor content was determined to be important in this case. Figure 20 is a schematic of the closed flow system. Water vapor absorption measurements at 9-11μm (CO_2 laser) are plagued with parasitic impurities. Strong contributions of ammonia, carbon dioxide, and at least two distinct hydrocarbons have been identified. These have been traced partly to the water sample (deionized) and partly to plastic tubing and connections. To eliminate the contaminants, nonmetallic elements were removed from the system except for teflon and mylar in the microphone and O-rings. The deionized water was then distilled several times in a small closed cycle system purged with an inert gas. This still was designed and constructed entirely of glass especially for this purpose. Distillations were performed over sulfuric acid and permanganates to remove the carbon dioxide and ammonia. A small glass flask with a glass-to-metal seal attached to a stainless steel bellows value was constructed to hold the purified water sample. All glass was etched and baked. Although traces of the ammonia absorption have not been entirely removed, the improved system yields values which reveal no other contaminants. This example indicates the care which may be required to obtain absorption coefficient values characteristic of the desired absorber. In such cases, the mass spectrometer gas analyzer is useless because the contaminant partial pressures are typically in the ppb (or less) range.

CW-Source Thermodynamic Equilibrium Type Differential Spectrophone

Two-chambered differential spectrophones with a signal passband at near 0 Hz were discussed previously. Because these spectrophones operate at near thermodynamic (though not adiabatic) equilibrium, they provide a useful comparison with those having an acoustical equilibrium. Signal linearity with total pressure in particular, which is clearly a good approximation for the differential system, may not be assumed for the acoustical system. Therefore, normalization can be provided by, for example, White cell measurements and/or the differential system. This may be accomplished on a one-time basis by using a single line comparison for all trace gas absorption measurements with an 80%/20%, N_2/O_2 buffer. The balanced differential spectrophone would also be ideally suited to absorption measurements for gases having relaxation rates into translation states that are near to or even lower than practical spectrophone resonance frequencies.

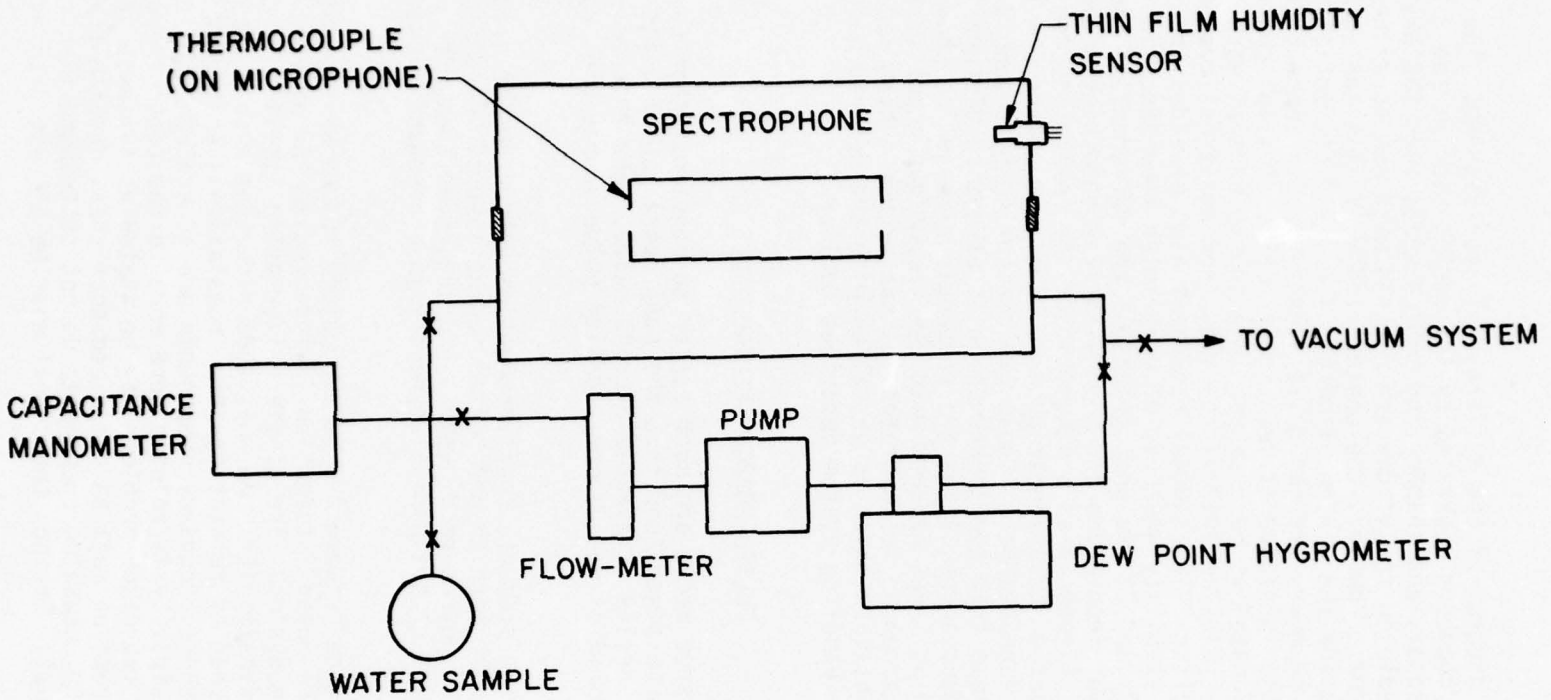

Figure 20. CW source water vapor spectrophone system.

Figure 21 shows a diagram of the differential spectrophone. The two identical, series chambers separated by the center window, the differential pressure sensor, and chamber and tubing walls form the basic system. Vacuum seals on the window are O-rings with one on either side of the center window. However, the center window is also sealed by another O-ring outside the window diameter, i.e., a differential seal. Note that the two chambers are not quite identical with respect to radiation though the imbalance is relatively small. The gas control valves have been located as near as possible to the ends of each chamber for even flushing. Similar thermal reservoir and antifrost systems have been described earlier. The thermal reservoir also provides greatly increased thermal stability which is of particular importance in this system. Figures 22 and 23 are photographs of the differential spectrophone, first without insulation and then with styrofoam packing and wooden casing installed. Figure 24 is a schematic of the control system constructed for support of this spectrophone. Pneumatic valves are located near both ends of each chamber. These are controlled by solenoid valves located some distance from the spectrophone so as not to disturb it. The four spectrophone access lines are presently siamesed as shown, and the two remaining lines connect with the vacuum/gas input system. Actually this spectrophone incorporates its own vacuum system and a stainless steel container which is prefilled with the desired gaseous mixture at the gas handling system described earlier.

PULSED-SOURCE SPECTROPHONES

Pulsed lasers for some media are much easier to construct than CW units since the pulsed pump power (and thus the pump rate) can be quite high while retaining an easily attainable average value. For this reason alone, the development of measurement quality pulse source spectrophones would be useful.

In the course of this project, spectrophones of unique design have been developed for use with both CW and pulsed source lasers. Consideration of the CW and pulsed source requirements had suggested that, for each, the same general kind of cylindrical symmetry in a resonant system would be appropriate.

The primary difference between the CW and pulsed source systems stems from the loss of the phase information (referenced to the driving source) in the single pulse system. The single driver pulse itself is a cause of reduced system sensitivity. An amplitude reduction also occurs since the pulse as broadened by relaxation into translational energy is coupled to acoustic modes whose frequency components are generally much lower. The problem of sensitivity is related here more to the total energy than to the power. The two major problems may be stated as follows. First, the physical construction must be optimized such that, despite the lack of phase selectivity, unwanted components do not contribute significantly to the ringing signal. Second, the signal must be processed so as to

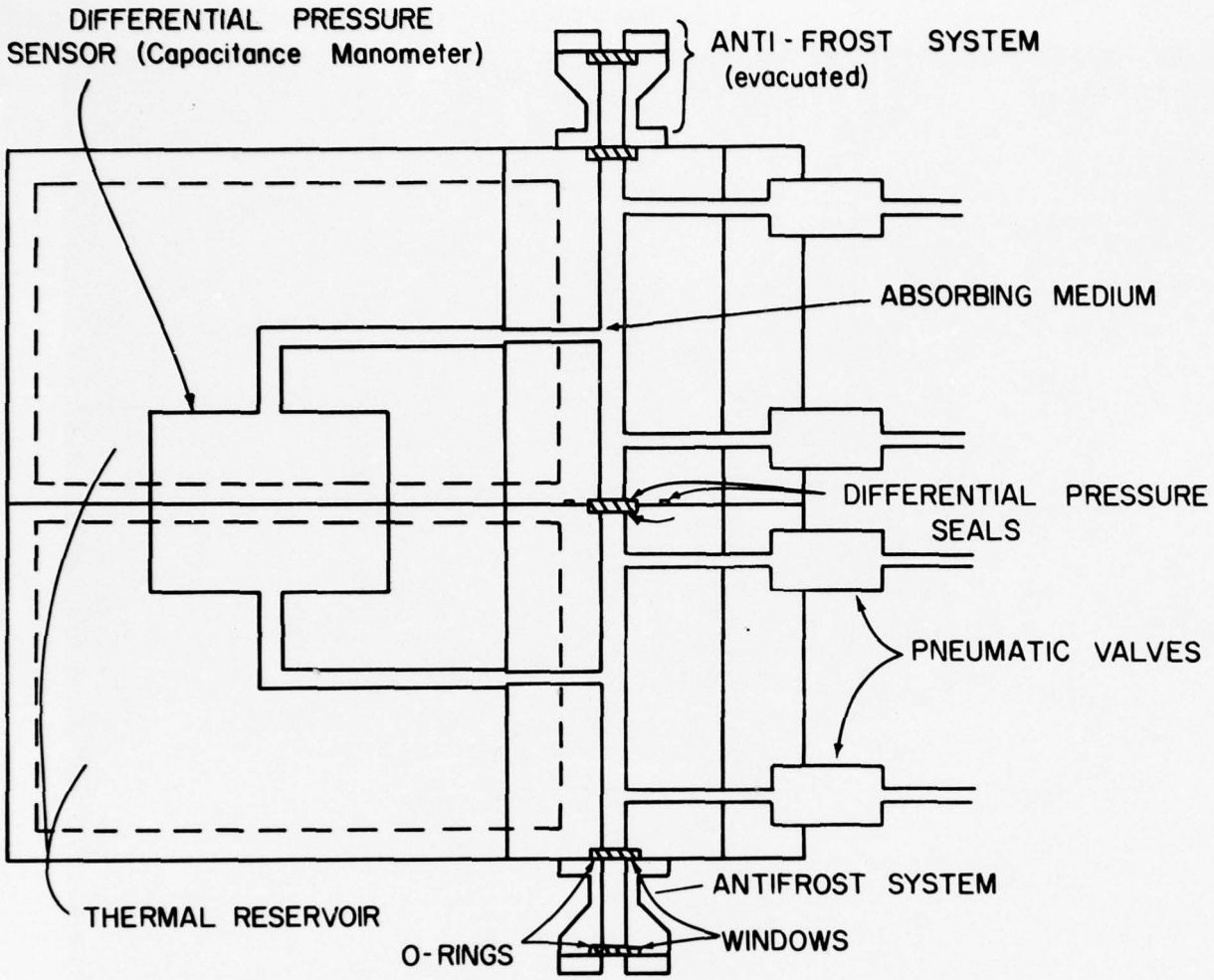

Figure 21. Diagram of CW source, differential spectrophone system.

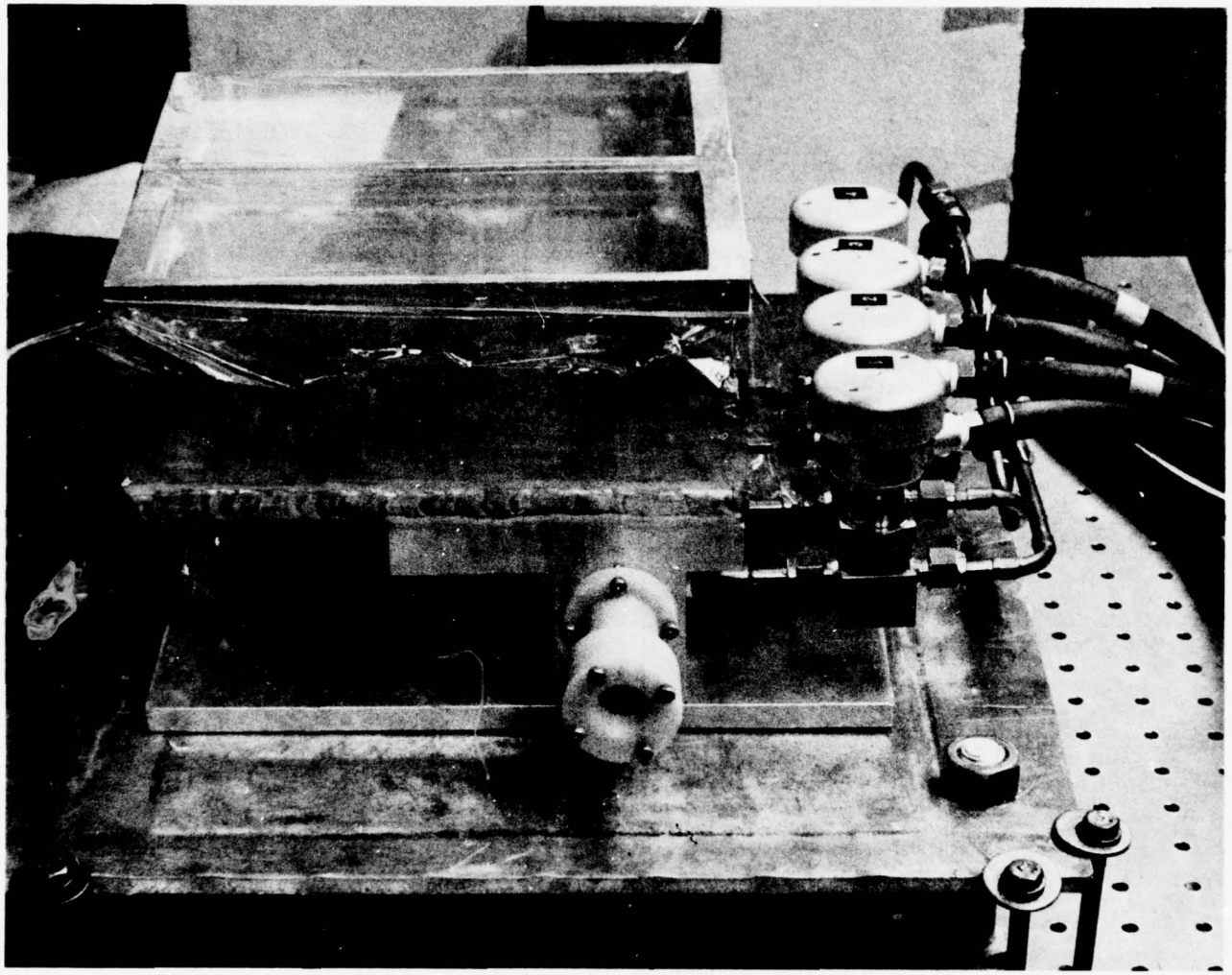

Figure 22. CW source differential spectrophone.

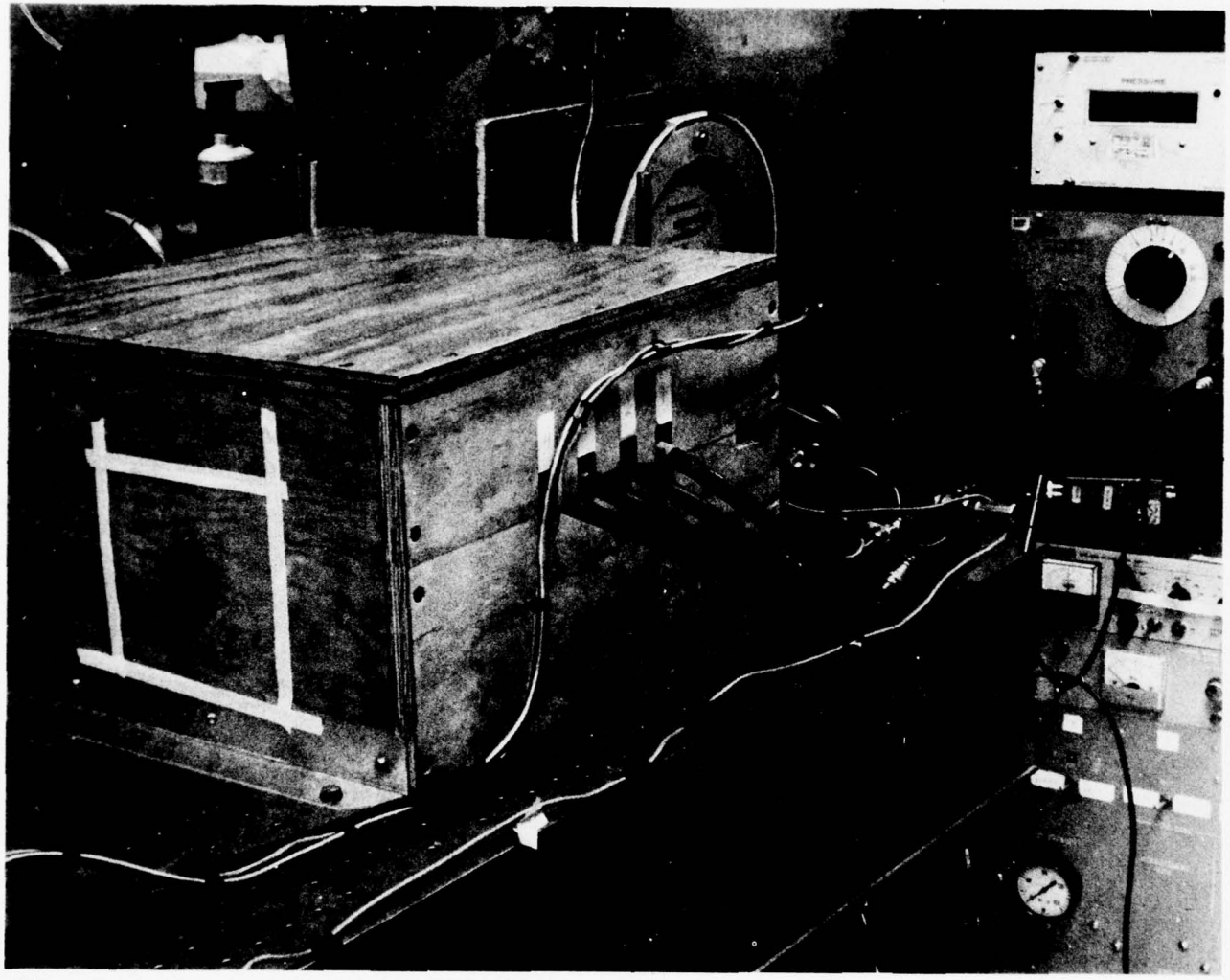

Figure 23. Thermal insulation applied to CW source differential spectrophone of Figure 22.

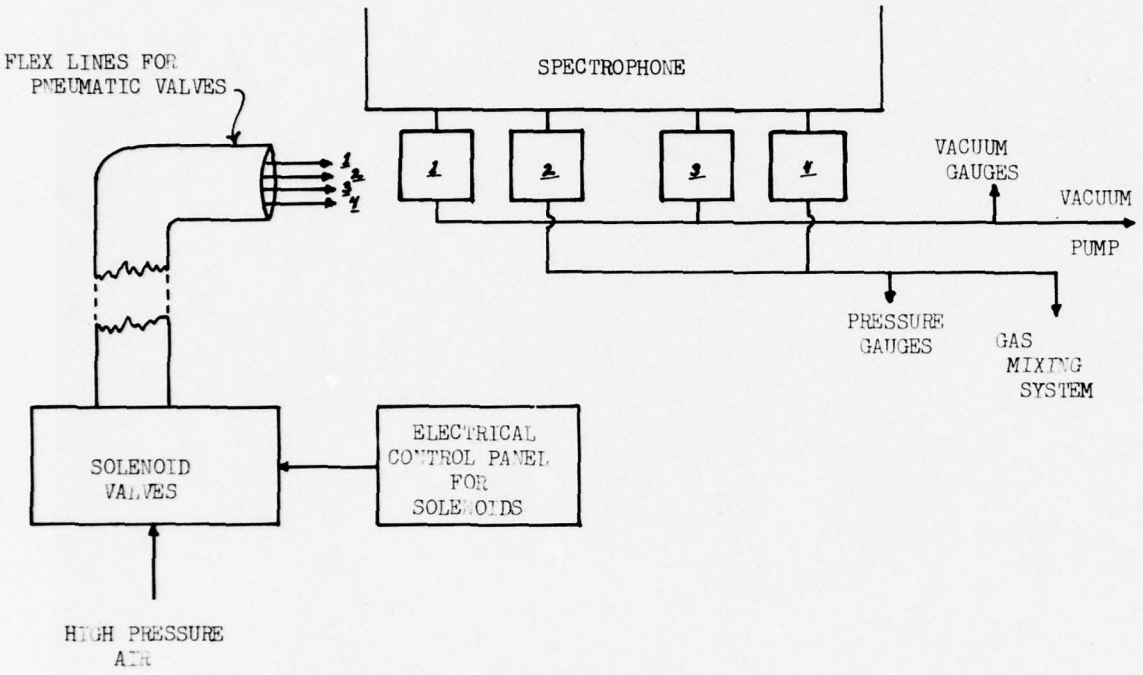

Figure 24. Control system for the differential spectrophone.

obtain narrowest possible bandwidth. Very high acoustical Q may be useful here, i.e., the filtering process may be initiated with a highly tuned acoustical system.

Figure 25 is a composite showing ringing results from: (a) a relatively high Q system (radial mode) and (b) a low Q (longitudinal mode) system. As can be seen, the purity of the modes in both cases is quite good. Q's obtained have ranged from 16 to about 800. Those of Fig. 25 are about 130 and 20 for upper and lower traces, respectively.

Some measurements with a pulsed source and which illustrate the basis for the physical designs have been performed. These have employed a spectrophone with a moveable end wall and both cylindrical section and end-wall microphones. Other smaller diameter, longitudinal wave, resonant systems having full cylindrical microphones have been also used.

The results were quite definite on the following points:

1. Coupling of either radial or longitudinal modes to either cylindrical or end-wall microphones was qualitatively close in magnitude. The sensors were essentially flush with the cavity surfaces.

2. Radial modes were dominant in the cavities of 4-inch and larger diameters and were virtually nonexistent in those 1-3/8-inch and smaller diameters - as expected. At this point it might be appropriate to mention that the radial frequency in the small bore systems has been purposely set very high, both to discourage coupling to these and to encourage purity of the longitudinal mode.

3. When the microphone consisted of a cylindrical section only and thus did not integrate around the radius, the reproducibility of the output signal was poor. When full cylindrical microphones were used, the reproducibility was good.

4. Linearity of the signal with total energy was verified.

Figures 26a, b, and c are examples of data pertaining to cylindrical section and full cylindrical microphones. In each case a number of traces are superimposed. Figure 26a shows results obtained with an end-wall microphone spectrophone of 4-inch diameter. These traces have not been normalized for laser pulse amplitude, but the variation for that quantity was generally less than 10%. The results of Fig. 26b represent the same conditions as Fig. 26a, but the microphone in this case is in the form of a cylindrical section subtending about a 60-degree angle from the center of the cylinder. The mode purity and reproducibility are both very poor here. This is admittedly an extreme example, but the interpretation that azimuthal dependence can be significant was supported by other measurements. In each case, however, reproducibility using complete

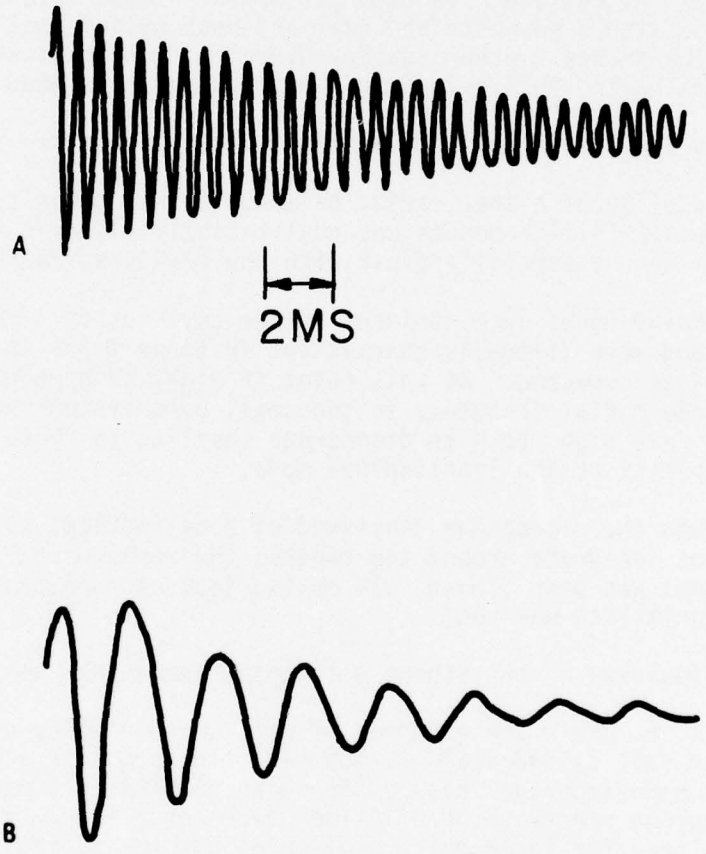

Figure 25. High and low Q pulsed spectrophone comparative results.

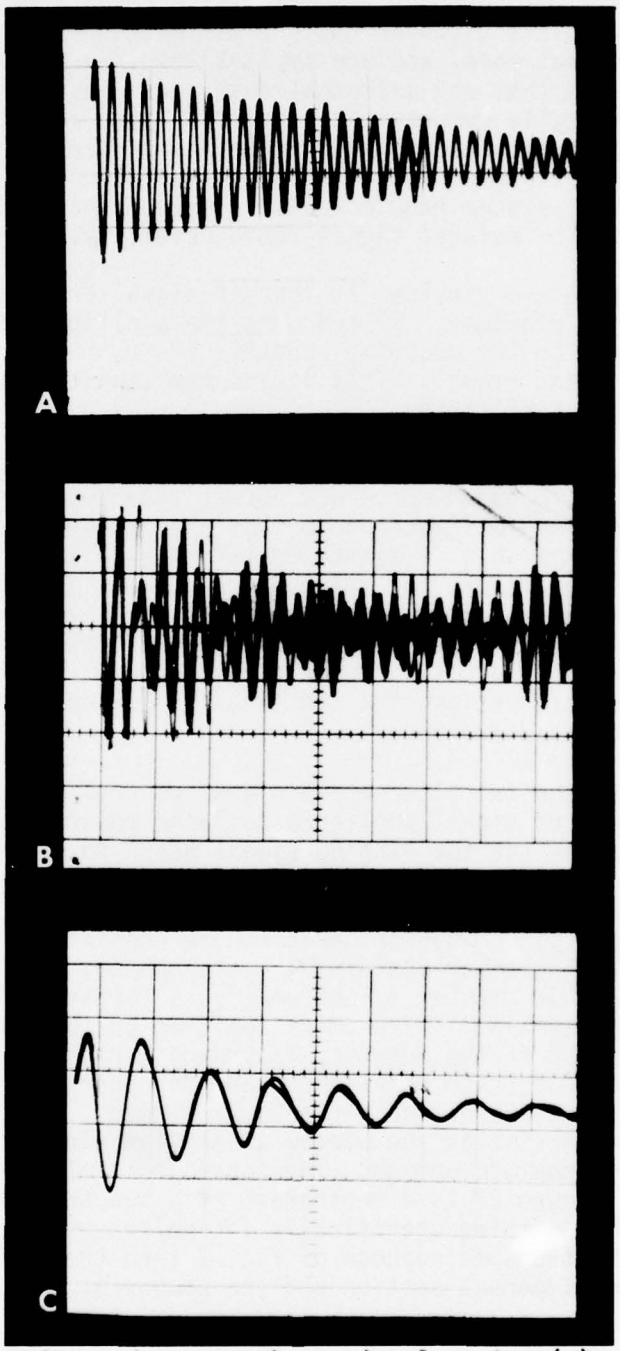

Figure 26. Superimposed spectrophone signals using (a) end-wall microphone, (b) 60-degree cylindrical section microphone, and (c) complete circular cylindrical microphone.

circular cylindrical microphones was good. The results of Fig. 26c were obtained with a complete circular cylindrical microphone having relatively low Q and longitudinal mode, and are typical results. A reason for this type of variation is that any azimuthal dependence must hinge on tenuous asymmetries in basically symmetrical systems. These results are given some attention since microphones used in resonant spectrophones often do not integrate over angle. This consideration which applies to both CW and pulsed source system requirements suggested that cylindrical symmetry would result in improved signal reproducibility.

The second of the design problems is that of signal processing when high sensitivity is required. If one uses the amplitude of, for example, the first full wave in the decaying acoustic train, the broadband noise is superimposed on the signal. This limits the sensitivity in spite of conventional bandpass filtering.

On the other hand, if one first transforms into the frequency domain, the signal and the broadband noise are effectively separated. High acoustical Q is particularly suited to this processing mode. The filtering effect of a typical high Q system expressed by use of the power spectrum is much higher than for available bandpass filters. The magnitude squared or power spectrum for a ringing signal similar to that of Fig. 25a is shown in Fig. 27. The ease of interpretation is improved. This peak can easily be digitized as a single value. To adapt the measurement to low S/N ratios, the digitized value would be that selected at the resonance center frequency.

Figure 28 displays the two alternative signal processing routes, i.e., either simple ratio of signal amplitude to laser power or the ratio of signal spectral power (at the ringing signal peak) to laser power. Signal averaging may be used, particularly to improve the S/N in the former case.

Basically then, the pulsed source spectrophone consists of an acoustically resonant cylindrical chamber containing a microphone, also having cylindrical symmetry. This chamber is internal to a larger cell which is vacuum tight and bakeable. The beam is admitted to the inner chamber through apertures and to the outer cell through barium fluoride end windows. Between each of these end windows and the apertures to the inner cell are acoustically dispersive elements or dampers. These dampers minimize the transmission of the window absorption signals into the chamber containing the microphone. The capacitance microphones have also been described. Figure 29 is a photograph of a spectrophone designed with dispersion and damping specifically for pulsed source use. Basically, this is similar to the spectrophone of Fig. 7 (and the Fig. 29 inset), but the length of the dispersal section and the number of damping discs were increased.

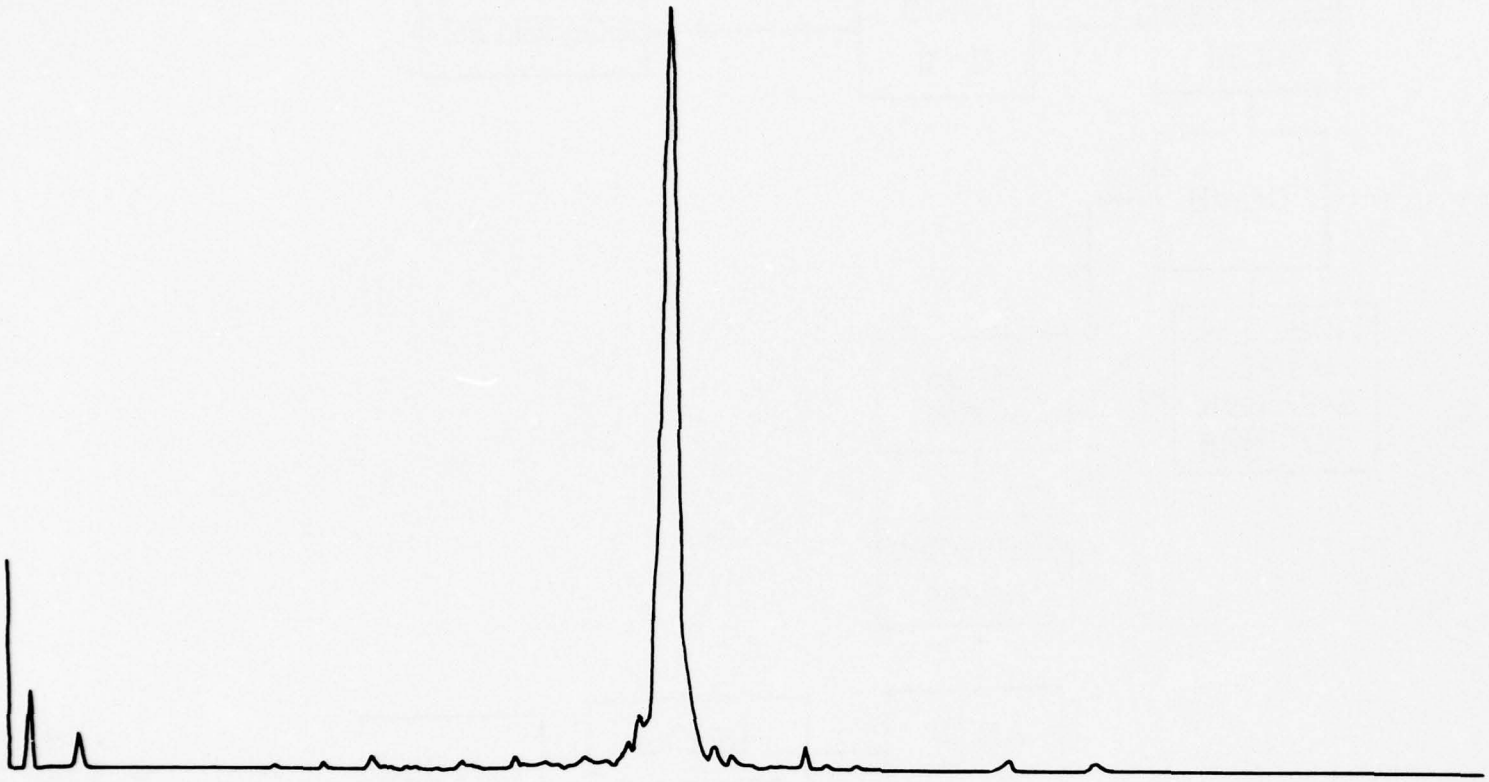

Figure 27. Power spectrum for ringing signal of Figure 25a.

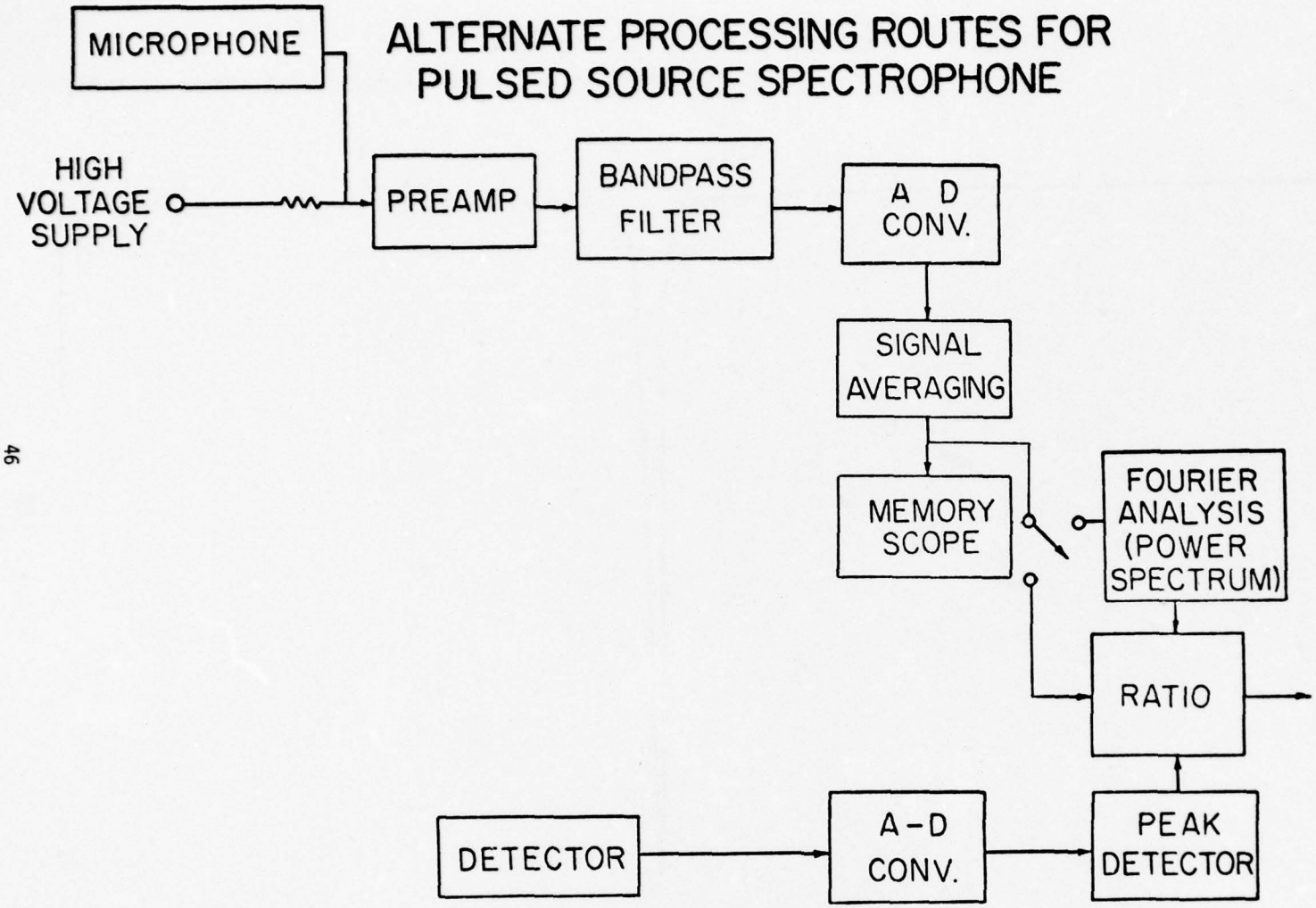

Figure 28. Alternative signal processing routes for pulse source spectrophone.

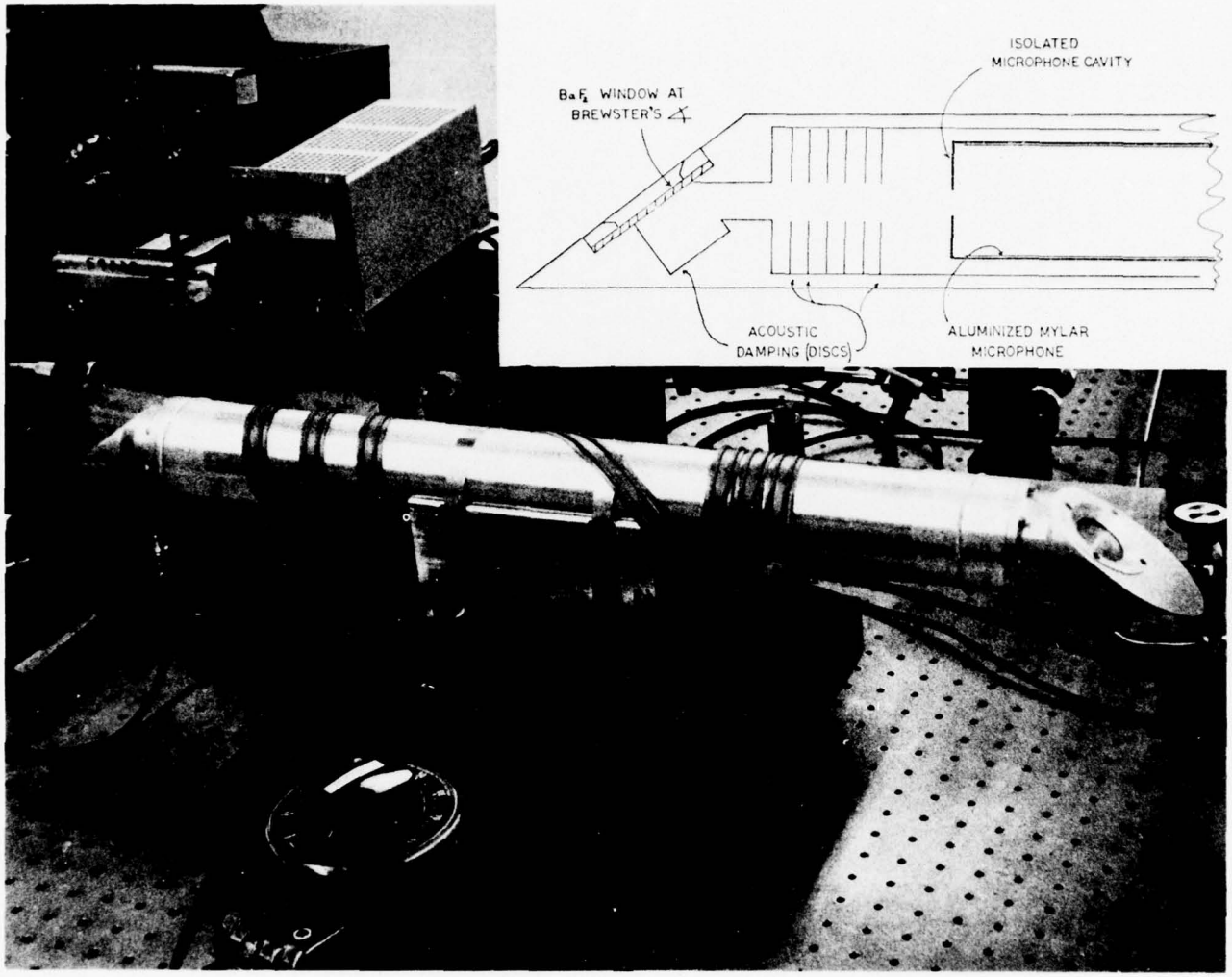

Figure 29. Longitudinal wave spectrophone designed for pulsed-source use, with diagram inset.

Pattern agreement for the pulsed source spectrophone data with the best of existing results was examined as it was for the CW source spectrophones. Figure 30 shows comparative results when a longitudinal mode, low Q spectrophone was used for absorption by methane at deuterium fluoride (DF) laser wavelengths. The primary comparison in this case is with White cell results also obtained at ASL [17]. Though on this relatively coarse plot the comparison appears very good, the differences for normalized pattern values ranged from 3% to 13.8% with no trends with amplitude of absorption value or frequency. The reproducibility of the energy detector used for this set of measurements was found to be 8% after calibration to remove a wavelength dependence. However, when compared with several other sets of values reported recently including White cell results, differential spectrophone results, and AFGL high resolution predictions, the ASL results are in much closer pattern agreement.

PULSED-SOURCE WATER VAPOR SPECTROPHONES

While the pulsed source spectrophone used for the methane measurements was of similar design to several used for CW source measurements, two more specialized systems have been constructed for water vapor and other absorbtion measurements at DF laser wavelengths using the same pulsed source. The primary motivation for these designs was increased system purity; therefore, both systems were constructed of stainless steel. Both systems were also fitted with continuous flow circuits for mixing and internal measurement of temperature, total pressure, and relative humidity.

One of these two spectrophones, a resonant, high Q system, was designed to tap the radial modes. It can be seen from the symmetry that the modes which are most directly excited by the expanding acoustic waves are radial in nature. In this case the diameter (8 inches) is much larger than for the longitudinal mode systems. Figures 31 and 32 are a cutaway drawing and a photograph, respectively, of the radial mode, pulsed source spectrophone. The Q of this system is about 800.

The second system (low Q) is dimensionally unchanged from the previous pulsed source longitudinal mode system.

These designs appear to have dealt successfully with the problems of slow mixing and contamination of the water samples as well as the more basic concern of sensitivity. The longitudinal mode system is relatively inexpensive, with analog signal averaging (no Fourier analysis required), simple to use, and compact. There is no trace of the so-called window signal, and measurements are routinely made at 10^{-2} (km^{-1}) using pulse energies of as low as 3 millijoules (~3 x 10^{-7} sec duration). The S/N ratio is generally between 20 and 40 dB at these levels; therefore,

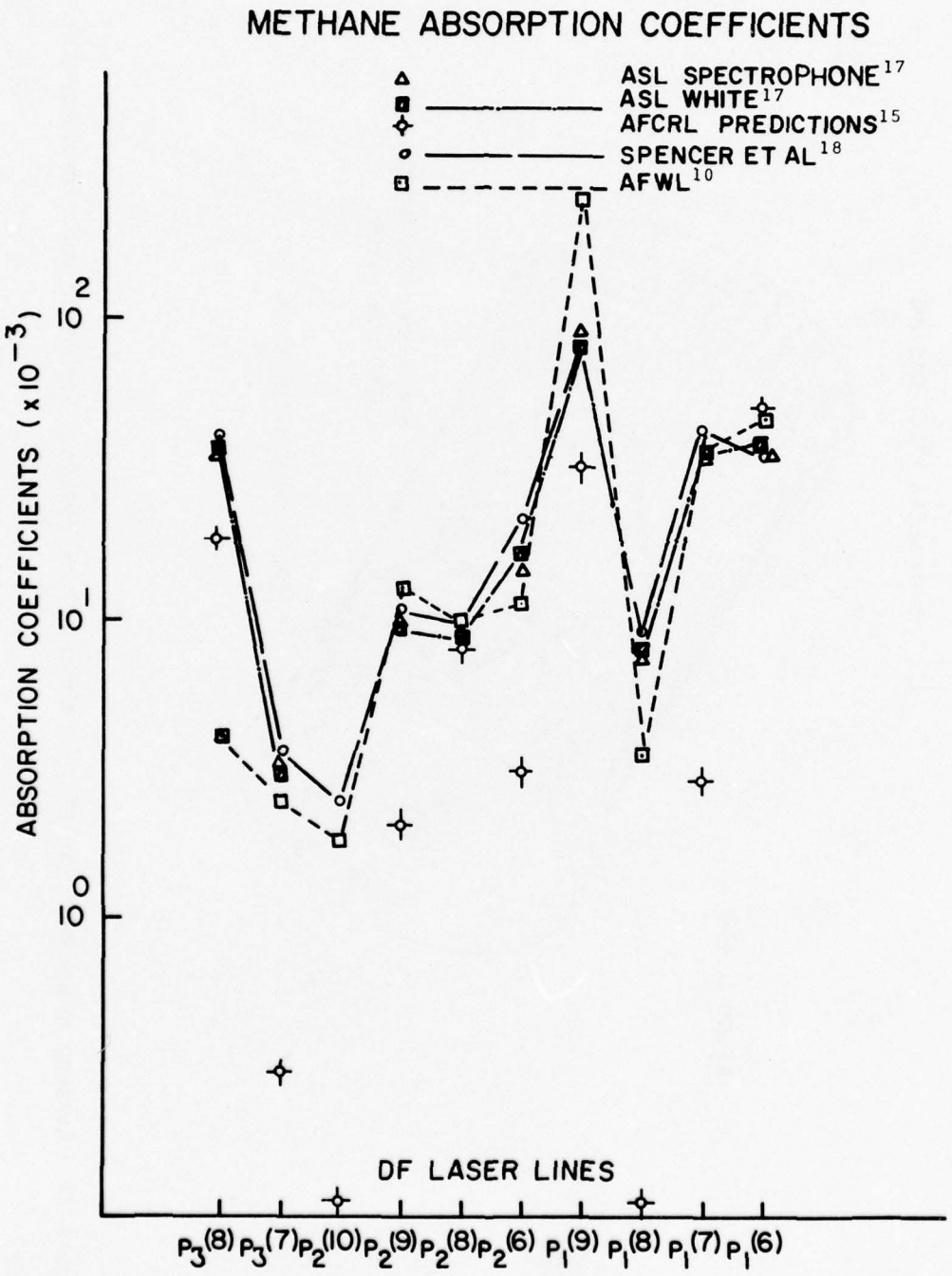

Figure 30. Comparative spectrophone and White cell results. Methane absorption coefficients are plotted for 9 DF laser wavelengths.

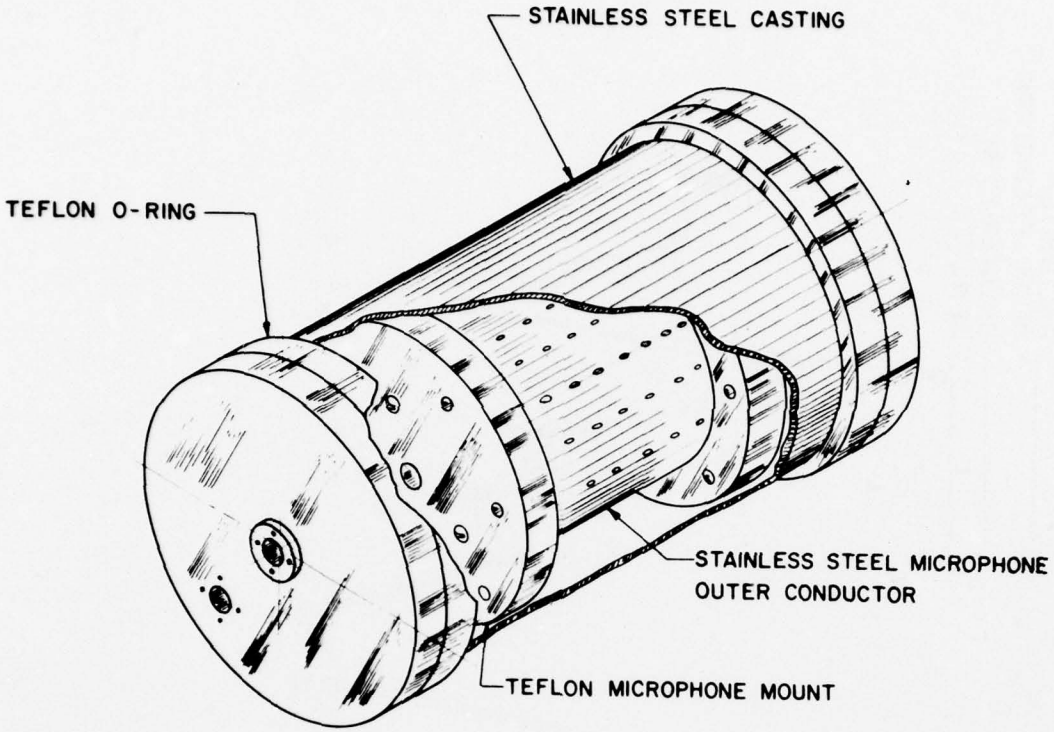

Figure 31. Cutaway drawing of radial mode spectrophone designed for water vapor measurements.

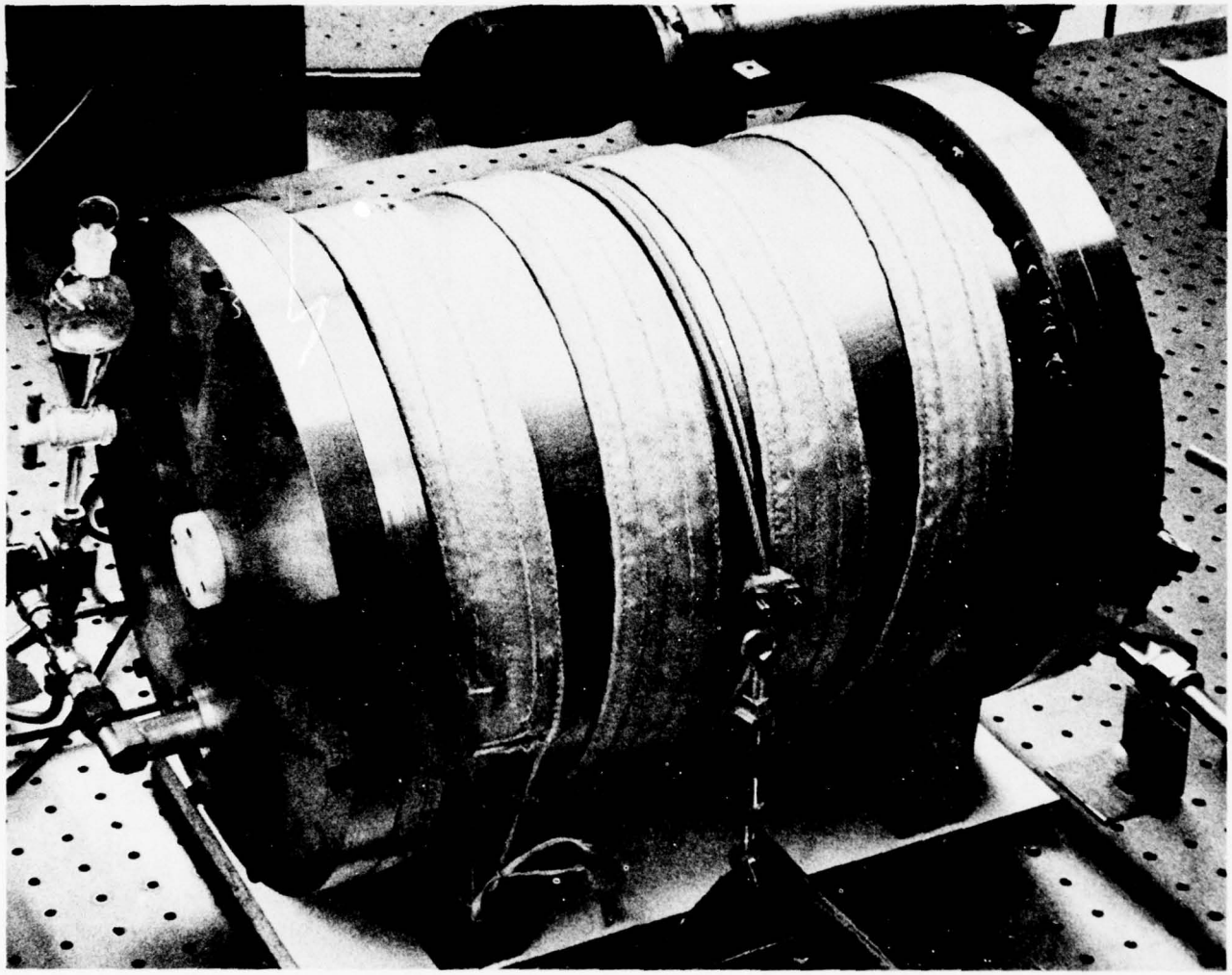

Figure 32. Radial mode water vapor spectrophone.

sensitivity for the present system is adequate for measurements at the 10^{-3} level though the threshold has not been sought. Of course, an increase in laser energy would provide a proportional increase in sensitivity. Either of these systems is well suited to the baking and pumping processes which precede sensitive measurements of absorption.

RESONANT SPECTROPHONES FOR IN-SITU ATMOSPHERIC MEASUREMENTS

Since the CW resonant systems described phase select the absorption signal from other contributions, they may be used windowless and open to the atmosphere. Sensitivity studies have been performed at CO_2 laser wavelengths, and more than adequate sensitivity exists for either gases or particulate absorption measurements. Water vapor (generally the dominant absorber) absorbs roughly 10% (km^{-1}) in general and much more at some laser line frequencies. Particulate absorption is often less but still measurable with the better than 10^{-3} km^{-1} available.

Armed with known absorption coefficients, concentrations of gaseous constitutients and absorption by particulate concentrations can be measured. Significant absorption occurs at CO_2 laser wavelengths (roughly 9.2-9.7μ and 10.2-10.7μ) by such gases as CH_4, O_3, NH_3, CO_2, as well as water.

The current model in-situ system is a vertically oriented resonant system with an intake horn at the upper end and a vacuum pump and flowmeter connected to the bottom.

RESONANT, DIFFERENTIAL SPECTROPHONE FOR IN-SITU GASEOUS AND/OR PARTICULATE ABSORPTION MEASUREMENTS

This system uses two series audio frequency, resonant spectrophones to measure in-situ, atmospheric particulate, and gaseous absorption contributions.

The system will also measure the gaseous contributions, as shown in the schematic diagram of Fig. 33. The two microphone signals, phase locked with respect to the laser beam, are fed into the differential lock-in amplifier. Initially, no filter is used and the output amplitude is peaked by using the phase corrector. In truth, this device is not generally needed (phase difference between signals is approximately zero). The attenuator is then adjusted to give a zero amplitude output. The filter is then inserted, and the A-minus-B signal then yields the particulates absorption signal. The total signal is generally much larger. The A signal input is grounded and the B signal is then the larger gaseous contribution. Figure 34 is a photograph of the operational system. Preliminary measurements made with this system tend to confirm the practicality of the data. However, since large particles do not follow gaseous streamlines, the calibration cycle is performed with the end windows removed

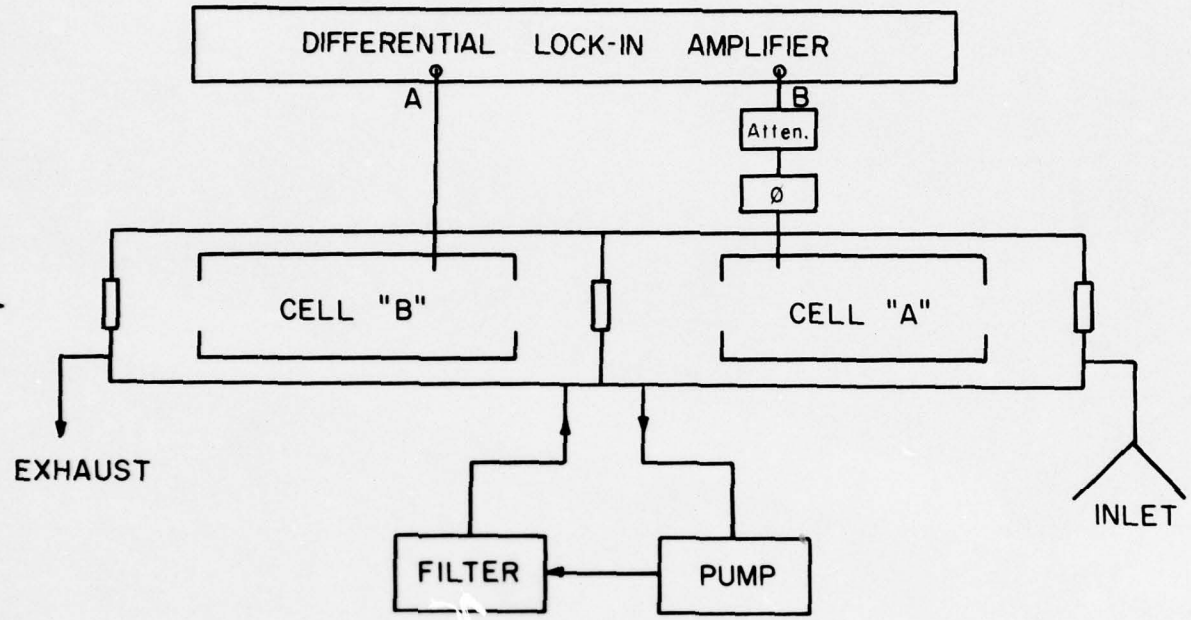

Figure 33. Schematic of resonant differential spectrophone for in-situ atmospheric measurements.

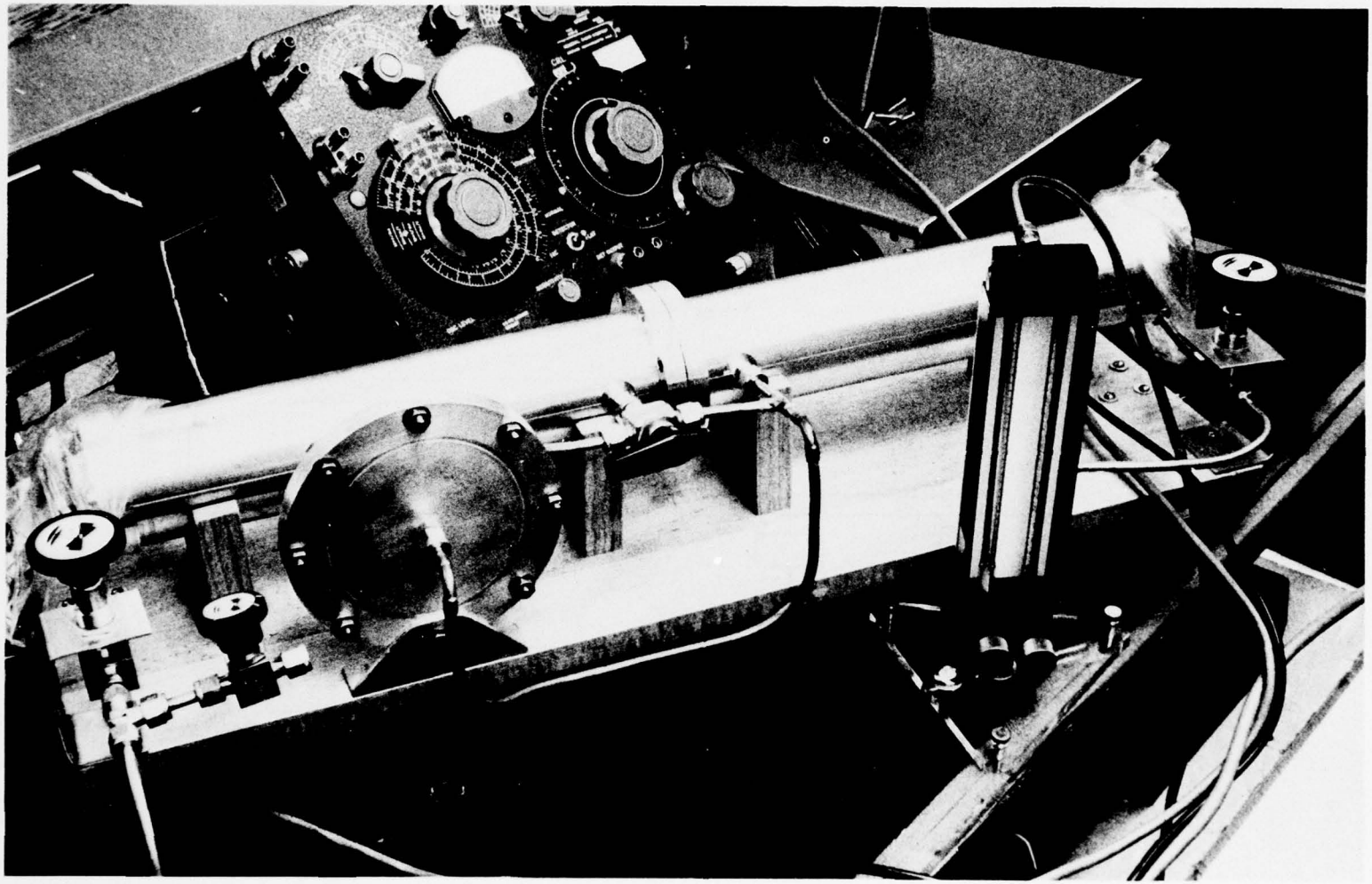

Figure 34. Photograph of the system of Figure 33.

(center window in place) and the vacuum pumping is done from the center. Thus, complete symmetry in the absorption is maintained. For differential operation, the two microphones are flow-connected in series.

CONCLUSIONS

Spectrophones appear to be well suited to high sensitivity absorption measurements. The resonant subsystems developed at the ASL have proven highly flexible as evidenced by the spectrum of applications which are discussed in this report. CW source applications had, of course, been reported earlier, though the resonant subchamber concept and the subsystem designs (e.g., microphone, antifrost, etc.) are new here. The development of a high sensitivity and measurement quality pulse source spectrophone is also new. These systems have been applied to a variety of IR absorption measurement problems including that of separating and quantifying gaseous and particulate absorption. The latter is also innovative, particularly in the form of the differential resonant spectrophone.

It should be mentioned, however, that neither the thermodynamic equilibrium (TE) type differential spectrophone nor any of the resonant systems described require a narrowband radiation source. In fact, a broader band source will simply result in a wavelength integrated, absorption measurement. A broadband source used with either resonant or TE differential spectrophones and a particular trace absorber in the "reference" side may be calibrated to yield a concentration for the test sample (same buffer) in the other half of the spectrophone. This may be calibrated as a concentration measurement in addition to providing absorption for the broadband sensors which are so prolific in current and anticipated defense systems.

REFERENCES

1. Bell, A. G., 1880, Proc. Am. Assoc. Advance Sci., 29, 115.

2. Tyndall, T., 1880, Proc. Roy Soc. (London A), 31, 307.

3. Kerr, E. L. and J. G. Attwood, 1968, "The Laser Illuminated Absorptivity Spectrophone: A Method for Measurement of Weak Absorptivity in Gases at Laser Wavelengths," Appl. Opt., 7, 915.

4. Trasty, G. L., 1973, "Absorption Measurements of the 10.4 micron Region Using a CO_2 Laser and a Spectrophone," Technical Report AFAL-TR-72-413 (Air Force Laboratory, Wright Patterson Air Force Base, OH.

5. Kreutzer, L. B., 1971, "Ultralow Gas Concentration Infrared Absorption Spectroscopy," J. Appl. Phys., 42, 2934.

6. Dewey Jr., C. F., R. D. Kamm, and C. E. Hackett, 1973, "Acoustic Amplifier for Detection of Atmospheric Pollutants," Appl. Phys. Lett., 23, 623.

7. Patel, C. K. N., 1974, "Spectroscopic Measurements of Stratospheric Nitric Oxide and Water Vapor," Science, 184, 1173.

8. Rosencwaig, A., 1973, "Photoacoustic Spectroscopy of Biological Materials," Science, 181, 657.

9. Rosengren, L., 1975, "Optimal Optoacoustic Detector Design," Appl. Opt., 14, 1960.

10. Deaton, T. F., D. A. Depatie, and T. W. Walker, 1975, "Absorption Coefficient Measurements of Nitrous Oxide and Methane at DF Laser Wavelengths," Appl. Phys. Lett., 26, 300.

11. Depatie, D. A., (unpublished).

12. Gordon, R. G. and R. P. McGinnis, 1968, J. Chem. Phys., 49, 2455.

13. Gordon, R. G. and R. P. McGinnis, 1971, J. Chem. Phys., 55, 4898.

14. Morse, P. M., 1936, Vibration and Sound (McGraw-Hill, NY).

15. McClatchey, R. A., W. S. Benedict, S. A. Clough, D. E. Burch, R. E. Calfee, F. Fox, L. S. Rothman, and J. S. Garing, 1973, "AFCRL Atmospheric Absorption Line Parameter Compilation," Air Force Cambridge Research Laboratories, Hanscom AFB, MA, AFCRL-TR-73-0096.

16. Patty, R. R., 1974, "CO_2 Laser Absorption Coefficients for Determining Ambient Levels of O_2, N H_3, and CH_4," Appl. Opt., 13, 2850.

17. Bruce, C. W., B. Sojka, R. Hurd, Z. Derzko, W. Watkins, and K. O. White, "Application of Pulsed-Source Spectrophones to Absorption by Methane at DF Laser Wavelengths," (to be published).

18. Spencer, D. J., G. C. Denault, and H. H. Takimoto, 1974, "Atmospheric Gas Absorption at DF Laser Wavelengths," Appl. Opt., 13, 2855.

ATMOSPHERIC SCIENCES RESEARCH PAPERS

1. Lindberg, J.D., "An Improvement to a Method for Measuring the Absorption Coefficient of Atmospheric Dust and other Strongly Absorbing Powders," ECOM-5565, July 1975.
2. Avara, Elton, P., "Mesoscale Wind Shears Derived from Thermal Winds," ECOM-5566, July 1975.
3. Gomez, Richard B. and Joseph H. Pierluissi, "Incomplete Gamma Function Approximation for King's Strong-Line Transmittance Model," ECOM-5567, July 1975.
4. Blanco, A.J. and B.F. Engebos, "Ballistic Wind Weighting Functions for Tank Projectiles," ECOM-5568, August 1975.
5. Taylor, Fredrick J., Jack Smith, and Thomas H. Pries, "Crosswind Measurements through Pattern Recognition Techniques," ECOM-5569, July 1975.
6. Walters, D.L., "Crosswind Weighting Functions for Direct-Fire Projectiles," ECOM-5570, August 1975.
7. Duncan, Louis D., "An Improved Algorithm for the Iterated Minimal Information Solution for Remote Sounding of Temperature," ECOM-5571, August 1975.
8. Robbiani, Raymond L., "Tactical Field Demonstration of Mobile Weather Radar Set AN/TPS-41 at Fort Rucker, Alabama," ECOM-5572, August 1975.
9. Miers, B., G. Blackman, D. Langer, and N. Lorimier, "Analysis of SMS/GOES Film Data," ECOM-5573, September 1975.
10. Manquero, Carlos, Louis Duncan, and Rufus Bruce, "An Indication from Satellite Measurements of Atmospheric CO_2 Variability," ECOM-5574, September 1975.
11. Petracca, Carmine and James D. Lindberg, "Installation and Operation of an Atmospheric Particulate Collector," ECOM-5575, September 1975.
12. Avara, Elton P. and George Alexander, "Empirical Investigation of Three Iterative Methods for Inverting the Radiative Transfer Equation," ECOM-5576, October 1975.
13. Alexander, George D., "A Digital Data Acquisition Interface for the SMS Direct Readout Ground Station—Concept and Preliminary Design," ECOM-5577, October 1975.
14. Cantor, Israel, "Enhancement of Point Source Thermal Radiation Under Clouds in a Nonattenuating Medium," ECOM-5578, October 1975.
15. Norton, Colburn and Glenn Hoidale, "The Diurnal Variation of Mixing Height by Month over White Sands Missile Range, NM," ECOM-5579, November 1975.
16. Avara, Elton P., "On the Spectrum Analysis of Binary Data," ECOM-5580, November 1975.
17. Taylor, Fredrick J., Thomas H. Pries, and Chao-Huan Huang, "Optimal Wind Velocity Estimation," ECOM-5581, December 1975.
18. Avara, Elton P., "Some Effects of Autocorrelated and Cross-Correlated Noise on the Analysis of Variance," ECOM-5582, December 1975.
19. Gillespie, Patti S., R.L. Armstrong, and Kenneth O. White, "The Spectral Characteristics and Atmospheric CO_2 Absorption of the Ho^{+3}:YLF Laser at 2.05μm," ECOM-5583, December 1975.
20. Novlan, David J., "An Empirical Method of Forecasting Thunderstorms for the White Sands Missile Range," ECOM-5584, February 1976.
21. Avara, Elton P., "Randomization Effects in Hypothesis Testing with Autocorrelated Noise," ECOM-5585, February 1976.
22. Watkins, Wendell R., "Improvements in Long Path Absorption Cell Measurement," ECOM-5586, March 1976.

23. Thomas, Joe, George D. Alexander, and Marvin Dubbin, "SATTEL — An Army Dedicated Meteorological Telemetry System," ECOM-5587, March 1976.
24. Kennedy, Bruce W. and Delbert Bynum, "Army User Test Program for the RDT&E-XM-75 Meteorological Rocket," ECOM-5588, April 1976.
25. Barnett, Kenneth M., "A Description of the Artillery Meteorological Comparisons at White Sands Missile Range, October 1974 — December 1974 ('PASS' — Prototype Artillery [Meteorological] Subsystem)," ECOM-5589, April 1976.
26. Miller, Walter B., "Preliminary Analysis of Fall-of-Shot From Project 'PASS'," ECOM-5590, April 1976.
27. Avara, Elton P., "Error Analysis of Minimum Information and Smith's Direct Methods for Inverting the Radiative Transfer Equation," ECOM-5591, April 1976.
28. Yee, Young P., James D. Horn, and George Alexander, "Synoptic Thermal Wind Calculations from Radiosonde Observations Over the Southwestern United States," ECOM-5592, May 1976.
29. Duncan, Louis D. and Mary Ann Seagraves, "Applications of Empirical Corrections to NOAA-4 VTPR Observations," ECOM-5593, May 1976.
30. Miers, Bruce T. and Steve Weaver, "Applications of Meterological Satellite Data to Weather Sensitive Army Operations," ECOM-5594, May 1976.
31. Sharenow, Moses, "Redesign and Improvement of Balloon ML-566," ECOM-5595, June 1976.
32. Hansen, Frank V., "The Depth of the Surface Boundary Layer," ECOM-5596, June 1976.
33. Pinnick, R.G. and E.B. Stenmark, "Response Calculations for a Commercial Light-Scattering Aerosol Counter," ECOM-5597, July 1976.
34. Mason, J. and G.B. Hoidale, "Visibility as an Estimator of Infrared Transmittance," ECOM-5598, July 1976.
35. Bruce, Rufus E., Louis D. Duncan, and Joseph H. Pierluissi, "Experimental Study of the Relationship Between Radiosonde Temperatures and Radiometric-Area Temperatures," ECOM-5599, August 1976.
36. Duncan, Louis D., "Stratospheric Wind Shear Computed from Satellite Thermal Sounder Measurements," ECOM-5800, September 1976.
37. Taylor, F., P. Mohan, P. Joseph and T. Pries, "An All Digital Automated Wind Measurement System," ECOM-5801, September 1976.
38. Bruce, Charles, "Development of Spectrophones for CW and Pulsed Radiation Sources," ECOM-5802, September 1976.

DISTRIBUTION LIST

Commanding Officer
Picatinny Arsenal
ATTN: SARPA-TS-S, #59
Dover, NJ 07801

Commanding Officer
Harry Diamond Laboratory
ATTN: Library
2800 Powder Mill Road
Adelphi, MD 20783

Commander
US Army Electronics Command
ATTN: DRSEL-RD-D
Fort Monmouth, NJ 07703

Naval Surface Weapons Center
Code DT 21 (Ms. Greeley)
Dahlgren, VA 22448

Air Force Weapons Laboratory
ATTN: Technical Library (SUL)
Kirtland AFB, NM 87117

Director
US Army Engr Waterways Exper Sta
ATTN: Library Branch
Vicksburg, MS 39180

Commander
US Army Electronics Command
ATTN: DRSEL-CT-D
Fort Monmouth, NJ 07703

Meteorologist in Charge
Kwajalein Missile Range
PO Box 67
APO
San Francisco, CA 96555

Environmental Protection Agency
Meteorology Laboratory
Research Triangle Park, NC 27711

Chief, Technical Services Div
DCS/Aerospace Sciences
ATTN: AWS/DNTI
Scott AFB, IL 62225

Air Force Cambridge Rsch Labs
ATTN: LCH (A. S. Carten, Jr.)
Hanscom AFB
Bedford, MA 01731

Department of the Air Force
16WS/DO
Fort Monroe, VA 23651

Director
US Army Ballistic Research Lab
ATTN: DRXBR-AM
Aberdeen Proving Ground, MD 21005

Geophysics Division
Code 3250
Pacific Missile Test Center
Point Mugu, CA 93042

National Center for Atmos Res
NCAR Library
PO Box 3000
Boulder, CO 80303

William Peterson
Research Association
Utah State University, UNC 48
Logan, UT 84322

Commander
US Army Dugway Proving Ground
ATTN: MT-S
Dugway, UT 84022

Head, Rsch and Development Div (ESA-131)
Meteorological Department
Naval Weapons Engineering Support Act
Washington, DC 20374

Commander
US Army Electronics Command
ATTN: DRCDE-R
5001 Eisenhower Avenue
Alexandria, VA 22304

Marine Corps Dev & Educ Cmd
Development Center
ATTN: Cmd, Control, & Comm Div (C^3)
Quantico, VA 22134

Commander
US Army Electronics Command
ATTN: DRSEL-WL-D1
Fort Monmouth, NJ 07703

Commander
US Army Missile Command
ATTN: DRSMI-RFGA, B. W. Fowler
Redstone Arsenal, AL 35809

Dir of Dev & Engr
Defense Systems Div
ATTN: SAREA-DE-DDR
H. Tannenbaum
Edgewood Arsenal, APG, MD 21010

Mr. William A. Main
USDA Forest Service
1407 S. Harrison Road
East Lansing, MI 48823

Naval Surface Weapons Center
Technical Library and Information
Services Division
White Oak, Silver Spring, MD 20910

Dr. A. D. Belmont
Research Division
PO Box 1249
Control Data Corp
Minneapolis, MN 55440

Dir, Elec Tech and Devices Lab
US Army Electronics Command
ATTN: DRSEL-TL-D, Bldg 2700
Fort Monmouth, NJ 07703

Director
Development Center MCDEC
ATTN: Firepower Division
Quantico, VA 22134

Commander
US Army Proving Ground
ATTN: Technical Library, Bldg 2100
Yuma, AZ 85364

US Army Liaison Office
MIT-Lincoln Lab, Library A-082
PO Box 73
Lexington, MA 02173

Library-R-51-Tech Reports
Environmental Research Labs
NOAA
Boulder, CO 80302

Head, Atmospheric Research Section
National Science Foundation
1800 G. Street, NW
Washington, DC 20550

Commander
US Army Missile Command
ATTN: DRSMI-RR
Redstone Arsenal, AL 35809

Commandant
US Army Field Artillery School
ATTN: Met Division
Fort Sill, OK 73503

Meteorology Laboratory
AFCRL/LY
Hanscom AFB
Bedford, MA 01731

Commander
US Army Engineer Topographic Lab
(STINFO CENTER)
Fort Belvoir, VA 22060

Commander
US Army Missile Command
ATTN: DRSMI-RRA, Bldg 7770
Redstone Arsenal, AL 35809

Air Force Avionics Lab
ATTN: AFAL/TSR
Wright-Patterson AFB, Ohio 45433

Commander
US Army Electronics Command
ATTN: DRSEL-VL-D
Fort Monmouth, NJ 07703

Commander
USAICS
ATTN: ATSI-CTD-MS
Fort Huachuca, AZ 85613

E&R Center
Bureau of Reclamation
ATTN: Bldg 67, Code 1210
Denver, CO 80225

HQDA (DAEN-RDM/Dr. De Percin)
Forrestal Bldg
Washington, DC 20314

Commander
Air Force Weapons Laboratory
ATTN: AFWL/WE
Kirtland AFB, NM 87117

Commander
US Army Satellite Comm Agc
ATTN: DRCPM-SC-3
Fort Monmouth, NJ 07703

Commander
US Army Electronics Command
ATTN: DRSEL-MS-TI
Fort Monmouth, NJ 07703

Commander
US Army Electronics Command
ATTN: DRSEL-GG-TD
Fort Monmouth, NJ 07703

Dr. Robert Durrenberger
Dir, The Lab of Climatology
Arizona State University
Tempe, AZ 85281

Commander
Headquarters, Fort Huachuca
ATTN: Tech Ref Div
Fort Huachuca, AZ 85613

Field Artillery Consultants
1112 Becontree Drive
ATTN: COL Buntyn
Lawton, OK 73501

Commander
US Army Nuclear Agency
ATTN: ATCA-NAW
Building 12
Fort Bliss, TX 79916

Director
Atmospheric Physics & Chem Lab
Code 31, NOAA
Department of Commerce
Boulder, CO 80302

Dr. John L. Walsh
Code 5503
Navy Research Lab
Washington, DC 20375

Commander
US Army Air Defense School
ATTN: C&S Dept, MSLSCI Div
Fort Bliss, TX 79916

Director National Security Agency
ATTN: TDL (C513)
Fort George G. Meade, MD 20755

USAF EPAC/CBT (Stop 825)
ATTN: Mr. Burgmann
Scott AFB, IL 62225

Armament Dev & Test Center
ADTC (DLOSL)
Eglin AFB, Florida 32542

Commander
US Army Ballistic Rsch Labs
ATTN: DRXBR-IB
Aberdeen Proving Ground, MD 21005

Director
Naval Research Laboratory
Code 2627
Washington, DC 20375

Commander
Naval Elect Sys Cmd HQ
Code 51014
Washington, DC 20360

The Library of Congress
ATTN: Exchange & Gift Div
Washington, DC 20540
2

CO, US Army Tropic Test Center
ATTN: STETC-MO-A (Tech Lib)
APO New York 09827

Commander
Naval Electronics Lab Center
ATTN: Library
San Diego, CA 92152

Office, Asst Sec Army (R&D)
ATTN: Dep for Science & Tech
Hq, Department of the Army
Washington, DC 20310

Director
US Army Ballistic Research Lab
ATTN: DRXBR-AM, Dr. F. E. Niles
Aberdeen Proving Ground, MD 21005

Commander
Frankford Arsenal
ATTN: Library, K2400, Bldg 51-2
Philadelphia, PA 19137

Director
US Army Ballistic Research Lab
ATTN: DRXBR-XA-LB
Bldg 305
Aberdeen Proving Ground, MD 21005

Dir, US Naval Research Lab
Code 5530
Washington, DC 20375

Commander
Office of Naval Research
Code 460-M
Arlington, VA 22217

Commander
Naval Weather Service Command
Washington Navy Yard
Bldg 200, Code 304
Washington, DC 20374

Technical Processes Br
D823
Room 806, Libraries Div NOAA
8060 13th St
Silver Spring, MD 20910

The Environmental Rsch Institute of MI
ATTN: IRIA Library
PO Box 618
Ann Arbor, MI 48107

Redstone Scientific Info Center
ATTN: Chief, Documents
US Army Missile Command
Redstone Arsenal, AL 35809

Commander
Edgewood Arsenal
ATTN: SAREA-TS-L
Aberdeen Proving Ground, MD 21010

Sylvania Elec Sys Western Div
ATTN: Technical Reports Library
PO Box 205
Mountain View, CA 94040

Commander
US Army Security Agency
ATTN: IARD-OS
Arlington Hall Station
Arlington, VA 22212
2

President
US Army Field Artillery Board
Fort Sill, OK 73503

Commandant
US Army Field Artillery School
ATTN: ATSF-TA-R
Fort Sill, OK 73503

CO, USA Foreign Sci & Tech Center
ATTN: DRXST-ISI
220 7th Street, NE
Charlottesville, VA 22901

Commander, Naval Ship Sys Cmd
Technical Library, Rm 3 S-08
National Center No. 3
Washington, DC 20360

Commandant
US Army Signal School
ATTN: ATSN-CD-MS
Fort Gordon, GA 30905

Rome Air Development Center
ATTN: Documents Library
TILD (Bette Smith)
Griffiss Air Force Base, NY 13441

HQ, ESD/DRI/S-22
Hanscom AFB
MA 01731

Commander
Frankford Arsenal
ATTN: J. Helfrich PDSP 65-1
Philadelphia, PA 19137

Director
Defense Nuclear Agency
ATTN: Tech Library
Washington, DC 20305

Department of the Air Force
5WW/DOX
Langley AFB, VA 23665

Commander
US Army Missile Command
ATTN: DRSMI-RER (Mr. Haraway)
Redstone Arsenal, AL 35809

CPT Hugh Albers, Exec Sec
Interdept Committee on Atmos Sci
Fed Council for Sci & Tech
National Sci Foundation
Washington, DC 20550

US Army Research Office
ATTN: DRXRO-IP
PO Box 12211
Research Triangle Park, NC 27709

Commander
US Army Training & Doctrine Cmd
ATTN: ATCD-SC
Fort Monroe, VA 23651

Mil Assistant for Environmental Sciences
OAD (E & LS), 3D129
The Pentagon
Washington, DC 20301

Commander
Eustis Directorate
US Army Air Mobility R&D Lab
ATTN: Technical Library
Fort Eustis, VA 23604

National Weather Service
National Meteorological Center
World Weather Bldg - 5200 Auth Rd
ATTN: Mr. Quiroz
Washington, DC 20233

Commander
US Army Materiel Command
ATTN: DRCRD-SS (Mr. Andrew)
Alexandria, VA 22304

Commander
Frankford Arsenal
ATTN: SARFA-FCD-O, Bldg 201-2
Bridge & Tarcony Sts
Philadelphia, PA 19137

Inge Dirmhirn, Professor
Utah State University, UMC 48
Logan, UT 84322

Chief, Aerospace Environ Div
Code ES41
NASA
Marsnall Space Flight Center, AL 35802

Dr. Frank D. Eaton
PO Box 3038
University Station
Laramie, Wyoming 82071

Commander
US Army Arctic Test Center
ATTN: STEAC-OP-PL
APO Seattle 98733

Commander
US Army Electronics Command
ATTN: DRSEL-GS-H (Stevenson)
Fort Monmouth, NJ 07703

Commander
USACACDA
ATTN: ATCA-CCC-W
Fort Leavenworth, KS 66027

Commander
US Army Test & Eval Cmd
ATTN: DRSTE-FA
Aberdeen Proving Ground, MD 21005

Air Force Cambridge Rsch Labs
ATTN: LKI
L. G. Hanscom Field
Bedford, MA 01730

Director, Systems R&D Service
Federal Aviation Administration
ATTN: ARD-54
2100 Second Street, SW
Washington, DC 20590

USAFETAC/CB (Stop 825)
Scott AFB
IL 62225

Director
USAE Waterways Experiment Station
ATTN: Library
PO Box 631
Vicksburg, MS 39180

Defense Documentation Center
ATTN: DDC-TCA
Cameron Station (BLDG 5)
Alexandria, Virginia 22314
12

Commander
US Army Electronics Command
ATTN: DRSEL-CT-S
Fort Monmouth, NJ 07703

Commander
Holloman Air Force Base
6585 TG/WE
Holloman AFB, NM 88330

Commandant
USAFAS
ATTN: ATSF-CD-MT (Mr. Farmer)
Fort Sill, OK 73503
2

Commandant
USAFAS
ATTN: ATSF-CD-C (Mr. Shelton)
Fort Sill, OK 73503
2

Commander
US Army Electronics Command
ATTN: DRSEL-CT-S (Dr. Swingle)
Fort Monmouth, NJ 07703
3

☆ U.S. GOVERNMENT PRINTING OFFICE: 1976—677-344/59